UNIVERSITY OF GOTHENBURG

DEPARTMENT OF BIOLOGICAL AND ENVIRONMENTAL SCIENCES

University of Gothenburg

Department of Biological and Environmental Sciences

Mixture effect of Dexamethasone & Benzo[a]pyrene in the *poeciliopsis lucida* hepatocellular carcinoma (PLHC-1) cell line

Lorenz Valentin Karl

Supervisor: Malin Celander

Mechanisms of toxicity -
Chemical interactions in fish (CYP Lab)

Degree project for Master of Science (60 hec) with a major in Ecotoxicology
ES25XX, Degree project environmental science (Master) H21, 60 hec
Second cycle
Semester/year: Autumn – Spring/ 2021-2022
Supervisor: Malin Celander, Department of Biological and Environmental Sciences
Examiner: Thomas Backhaus, Department of Biological and Environmental Sciences

Acknowledgment

I want to thank all the members of the CYP lab for their input, feedback, and support during the time I was able to spend there and work on my project.

Specifically, I want to thank Annika Lindkvist for working along with me throughout the months and helping me to collect a representative amount of experimental data. Further I want to thank Maja Edenius for teaching me how to work with the cell line and perform the assays. Finally, I want to thank my supervisor Malin Celander who was always happy to discuss the newest developments in my project. Especially in the last few months before my presentation she was always quick to respond and eager to give feedback, despite her many other obligations especially concerning the organization of the PRIMO conference.

Abstract

At present days, inland water bodies and seashores show significant levels of various pharmaceuticals. This is to a great extent due to the low removal rate of common wastewater treatment plants when it comes to pharmaceuticals. As pharmaceuticals, dosed adequately, are perceived as harmless to humans, the concentrations of pharmaceuticals present in the environment are often not considered problematic. However, several aspects give a reason for concern. Besides the long-term effects of bioaccumulating pharmaceuticals and sensitive, highly-adaptive microorganisms, potential mixture effects are one of the most distressing concerns. While the toxic effects of single, isolated compounds may be known or easily assessable, the "cocktail" effect existing from chemical mixtures is significantly more difficult to predict and investigate. (Backhaus and Karlsson 2014; Lindim et al. 2019; Ukić et al. 2019; Wassmur et al. 2013). In this thesis, we focus on the interactions between two substances, Dexamethasone (DEX) and Benzo[a]pyrene (BaP) in the *poeciliopsis lucida* hepatocellular carcinoma (PLHC-I) cell line. We tested different mixture compositions to investigate GR-AhR crosstalk in these cells. Our study reveals increased CYP1A (EROD) activity (1.5 to 2-fold) in cells treated with a mixture of DEX and BaP, compared to cells treated with BaP only, whereas DEX alone, did not affect CYP1A induction. Interestingly, the difference in response was less prominent in cells exposed to BaP concentrations below 0.5 µM and in cells exposed to DEX concentrations greater than 2.5 µM. Time-course experiments showed that the synergistic mixture effect on CYP1A induction peaked at 48h after dosing with shorter exposure times showing lower CYP1A induction. To put the interaction between DEX and BaP into perspective, we tested three additional GR agonists and β-naphthoflavone (BNF) as an AhR agonist. Our results showed similar potentiating effects with all four GR agonists combined with the two AhR agonists on CYP1A induction. Our findings confirm previous studies showing exposure to mixtures of GR- and AhR agonists having potentiating effects on CYP1A induction (Celander et al. 1997; Wassmur et al. 2013). By testing several glucocorticoids in combination with two different AhR agonists, we demonstrated that there is consistent GR-AhR crosstalk on CYP1A induction in this fish cell line.

Keywords: *Benzo[a]pyrene, Dexamethasone, CYP1A, chemical mixtures, PLHC-I, GR-AhR crosstalk*

Pharmaceuticals change how fish react to toxic substances.

Environmental pollution is a growing problem all around the globe. Even in industrial countries with high standards in waste treatment, contaminants like plastics and pharmaceuticals can be found even in the remotest of places. The potential severity of environmental contamination is to a great extent unknown. Flora and fauna are exposed to a smorgasbord of different pollutants, which gives reason to concern about what combined effect these substances have on the environment. The effects single compounds have on different organisms can be easily tested with state-of-the-art techniques and are well studied for the most prominent pollutants. However, it gets exponentially more complicated the more substances are involved.

In this thesis, I discuss the effects of two fundamentally different classes of substances and how they behave when applied in a mixture. First, benzo[a]pyrene (BaP), which belongs to the group of aryl hydrocarbons, is a common, pro-carcinogenic, pollutant that exists from organic combustion and can be detected in areas all around the globe. Secondly, dexamethasone (DEX), which belongs to the group of the glucocorticoids, is a pharmaceutical used as an active ingredient in a wide range of medications (for example in the treatment of cancer, lupus, arthritis and more recently in the treatment of Covid-19-patients. Most sewage treatment plants are not designed to filter out pharmaceuticals including DEX which are instead being released into the aquatic environment.

Although both substances act via different pathways in the cell, studies have shown that DEX can influence the response of liver cells to aryl hydrocarbons and similar acting substances. Most of these studies, were performed on mammalian cells. In my research, I used fish liver cells as a model organism as fish are much more exposed to BaP and DEX in the environment. I used different techniques (EROD assay, QPCR), to investigate the mixture effect from different angles, overall focussing on the changes in expression of the enzyme cytochrome P450 1A (CYP1A). This enzyme is responsible for the metabolism and elimination of compounds such as BaP. By changing parameters like exposure time of the cells, and concentration and composition of the mixture I attempt to learn more about how the substances interact. To put my findings into perspective, I tested different types of glucocorticoids and with β-naphthoflavone (BNF) a compound that behaves similar to BaP.

I was able to show that while DEX and the other glucocorticoids tested, did not increase the abundance of CYP1A when applied alone, they alter the expression of the enzyme when combined with AhR agonists. Depending on the composition of the mixture and the exposure duration, the response of the cells differs from the response to only BaP. This shows us that uptake of DEX alters how fish liver cells react to a toxicant such as BaP which can have serious, adverse effects on the species.

Table of Contents

List of Abbreviations

Table 1: List of Abbreviations.

Abbreviations	Names
AhR	Aryl hydrocarbon receptor
AhRE	Aryl hydrocarbon response element
AIP	AhR interacting protein
ARNT	Aryl hydrocarbon nuclear transporter
BaP	Benzo[a]pyrene
bHLH	Basic helix-loop-helix
BNF	β-napthoflavone
BM	Betamethasone
BSA	Bovine Serum Albumin
CA	Concentration Addition
cDNA	Complementary DNA
Cq-value	Cycle quantification value
C-Src	Cellular Sarcoma
CYP1A	Cytochrome P450 1A
DEX	Dexamethasone
DMSO	Dimethylsulfoxide
EDTA	Ethylenediaminetetracetic acid
ER	Estrogenic receptor
EROD	Ethoxy-resorufin-O-deethylase
FBS	Fetal Bovine Serum
GC-MS	Gas chromatography-mass spectrometry
gDNA	genomic DNA
GR	Glucocorticoid receptor
GRE	Glucocorticoid response element
HEPES	4-(2-hydroxyethyl)-1-piperazineethanesulfonic acid
HSP90	Heat shock protein 90
HYC	Hydrocortisone
IA	Independent Action
MEM	Minimum Essential Medium
MoA	Mode of Action
mRNA	messenger RNA
PAH	Polyaromatic hydrocarbon
PAS	Period/ARNT/Single-Minded
PBS	Phosphate Buffered Saline
PCB	Polychlorinated biphenyl
PCR	Polymerase chain reaction
PHAH	Polyhalogenated aromatic hydrocarbon
PHLC-I	*Poeciliopsis lucida* hepatocellular carcinoma I
POMC	Pro-opiomelanocortin
PRD	Prednisolone
SIM	Selective ion monitoring
TCDD	2,3,7,8-Tetrachlorodibenzodioxin
TIC	Total ion current chromatogram
qPCR	quantitative PCR
XAP 2	X-associated protein 2
XRE	Xenobiotic response element
3-MC	3-methylcholanthrene

1. Introduction

1.1 Aim

This thesis aims to assess a potential mixture effect of the glucocorticoid-receptor (GR) agonist dexamethasone with the aryl hydrocarbon receptor (AhR) agonist benzo[a]pyrene on the cytochrome P450 (CYP1A) biomarker response in a hepatic fish cell line (PLHC-1).

1.2 Mixture Toxicity

At present day, inland water bodies and seashores show significant levels of various pharmaceuticals. This is to a great extent due to the low removal rate of pharmaceuticals in common sewage water treatment plants that are therefore released into the aquatic environment. Although pharmaceuticals, when dosed adequately, are perceived as harmless to humans, the effects linked to exposure of non-target organisms to pharmaceuticals present in the environment are often less known.

Several aspects give reason for concern. One, regards the microbial community which in some cases is highly sensitive to pharmaceutical compounds and may quickly develop antibiotic immunity, resulting in a disturbance of the ecosystem. Also, although certain pharmaceuticals may not possess immediate, toxic characteristics at low concentrations, they can cause long-term effects due to bioaccumulation. Furthermore, these compounds that pass through the sewage water treatment plants into the surrounding aquatic environment, create a complex and challenging environment for living organisms.

While the toxic effects of single, isolated compounds may be known or easily assessable in the laboratory, the “cocktail” effect existing from chemical mixtures is significantly more difficult to predict and assess. (Backhaus and Karlsson 2014; Lindim et al. 2019; Ukić et al. 2019). There are well-established models, e.g., the concentration addition (CA) and the independent action (IA), to predict or at least approximate mixture toxicity. However, these models assume an additive mixture effect where the chemicals do not directly interact but have the same mode of action (MoA). Nevertheless, chemicals often interact in a way that results in an effect which is higher than the additive prediction, which is referred to as “synergistic” mixture effect (Fallahi et al. 2020).

This is true for interactions of certain pharmaceuticals with other, common environmental pollutants such as polycyclic aromatic hydrocarbons (PAHs) and other aromatic hydrocarbons. It has previously been described that the biological and biochemical effects of widespread, toxic contaminants like pyrene, BaP, and indenol[1,2,3cd]-pyrene, are influenced by pharmaceuticals like DEX. Although these compounds activate different cell receptors, *in vitro* experiments on the mammalian liver and ovarian cells have shown transactivation upon exposure to a mixture of such compounds (Wang et al. 2009).

1.3 Benzo[a]pyrene (BaP) and the aryl hydrocarbon receptor (AhR)

BaP (Figure 1) is a well-studied PAH that is widespread in the environment and known to act as a procarcinogen in humans. Although there is no known practical use and no intentional production of the substance, it is omnipresent, as it exists from various processes of organic combustion (Collins et al. 1991; Hattemer-Frey and Travis 1991). According to Collins et al. (1991), it is the most studied and most potent toxicant among the PAHs (Collins et al. 1991). As Kapitulnik et al. (1971) describe, the carcinogenic potential of BaP increases upon exposure. When BaP is transformed it yields carcinogenic metabolites such as BaP-7, 8-diol and BaP-9, 10-epoxide that pose to be even more toxic to bacterial and mammalian cells than BaP itself (Kapitulnik et al. 1977).

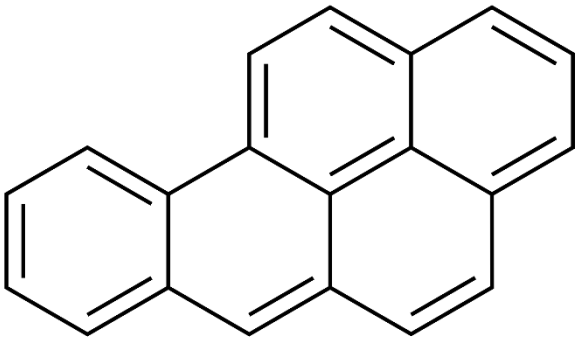

Figure 1: Chemical structure of Benzo[a]pyrene.

BaP binds to and activates the aryl hydrocarbon receptor (AhR) which is a target receptor for many environmental xenobiotics such as PAHs and planar halogenated aromatic hydrocarbons such as planar PCBs and dioxins. Upon binding, the AhR initiates the transcription of aromatic hydrocarbon-metabolizing enzymes such as cytochrome P450 (CYP) enzymes that facilitate the biotransformation and ultimately elimination of xenobiotic substances; in particular members of the CYP1A subfamily. Induction of CYP1A expression and/ or enzyme activity is therefore an established biomarker utilized to assess exposure to aromatic hydrocarbons in the environment.

The AhR is a member of the basic helix-loop-helix Period/ARNT/Single-Minded (bHLH-PAS) family and it is located in the cytoplasm (Larigot et al. 2018). When unbound in the cytoplasm, the AhR binds to two heat shock proteins (HSP90 proteins), the 23-kDa co-chaperone p23 and the immunophilin-like AhR interacting protein (AIP/XAP 2/ARA 9), to stabilize it. The complex further interacts with tyrosine kinase cellular sarcoma (c-Src) AIP, which protects it from degradation. Upon binding, the complex dissociates and tyrosine c-Src is released into the cytosol. The nuclear localization signal in the bHLH motif is uncovered and the complex is transported to the nucleus. To initiated transcription of the CYP1A gene, the complex binds to a xenobiotic-/Ah-responsive element (XRE/AhRE), a consensus sequence, occurring once or many-fold on the CYP1A gene of the respective organism. After initiating

transcription, the AhR complex is exported from the nucleus, ubiquitinated, and subsequently degraded by the 26S proteasome (Abel and Haarmann-Stemmann 2010; Hankinson 1995). Figure 2 shows a schematic of the AhR pathway.

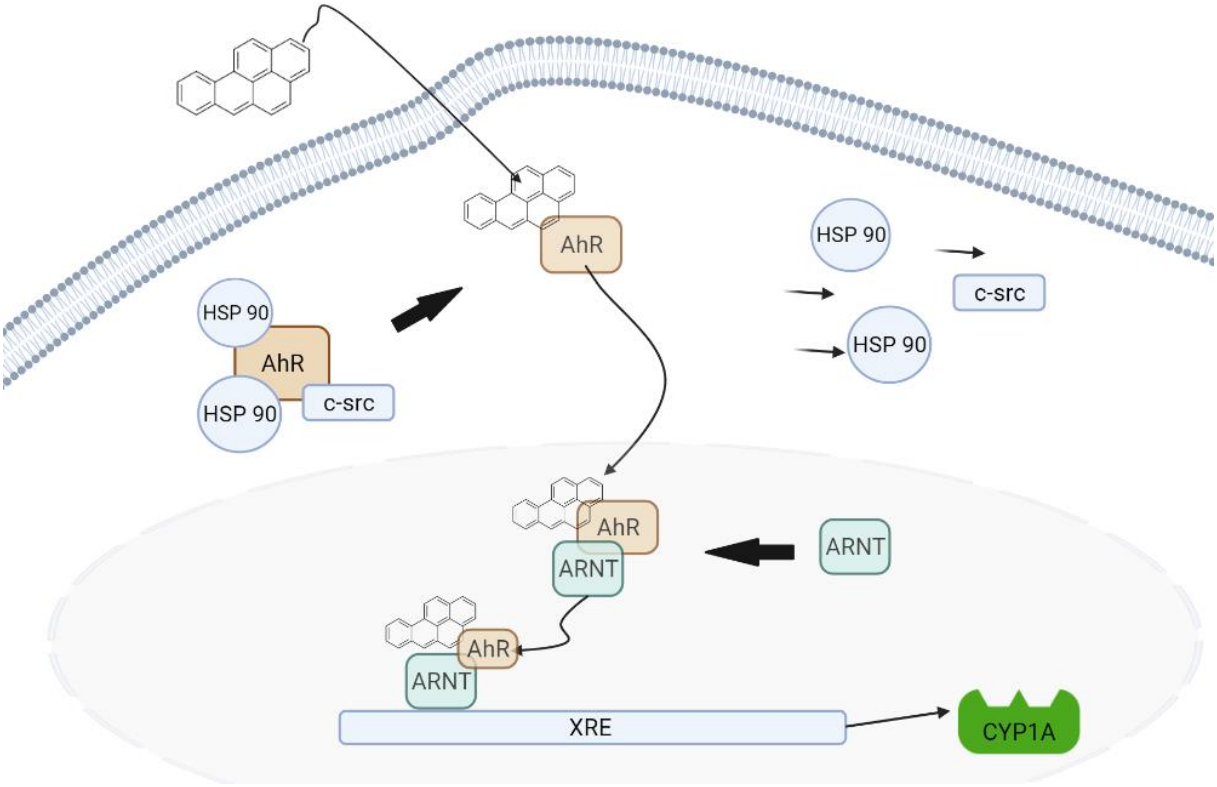

Figure 2: A simplified schematic of the AhR receptor pathway. The xenobiotic, in this case BaP, enters through the cell membrane and binds to the AhR receptor complex, that dissociates upon binding. The bound receptor transfers to the nucleus where it binds to the ARNT. The newly formed complex binds to the XRE where it initiates the transcription of CYP1A (Created with BioRender™).

1.4 Dexamethasone (DEX) and the glucocorticoid receptor (GR)

DEX (Figure 3) is a synthetic glucocorticoid (group of corticosteroids) that was developed as an anti-inflammatory agent and is also utilized in pharmacological products that treat various other diseases such as arthritis, lupus, breathing disorders, bacterial meningitis, and several types of cancer (Entringer S. 1996; McCracken and Lebel 1989; Yennurajalingam et al. 2013). As the Covid 19 pandemic was developing, DEX became a substance of interest as a potential candidate for therapy for people infected with the coronavirus (Lammers et al. 2020).

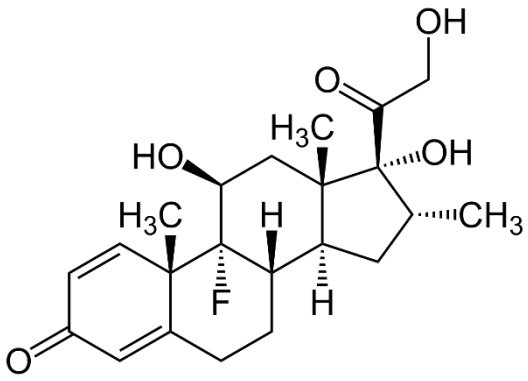

Figure 3: Chemical structure of Dexamethasone.

Ecotoxicological studies conducted on zebrafish showed that continuous exposure to DEX causes suppressed expression of the Pro-opiomelanocortin (POMC) hormone (EC50: 35 µM), which influences their stress response. Chronic exposure of the crustacean *Daphnia magna* has revealed inhibition of growth in crustaceans (EC50: 48.30 mg/ L (39.91-58.45), 95% confidence interval) (DellaGreca et al. 2004; Sun et al. 2010). While concentrations of DEX can exceed micromolar concentrations in hospital wastewater discharges, the concentrations detected in environmental matrices are usually in a low nanomolar range (Musee et al. 2021).

DEX alone has no effect on the CYP1A transcription; however, when combined with an AhR agonist, DEX enhances the activity of the AhR-CYP1A signalling in vertebrate hepatic cells which increase the production of CYP1A enzymes. DEX has been shown to influence the expression of CYP1A in various mammalian cells as well as fish cells when added together with PAHs or PHAHs (Celander et al. 1996; Pascussi et al. 2000). In addition, DEX also enhances the activity of the pregnane X receptor in human hepatocytes which increases the production of CYP3A enzymes. According to *Pascussi et al. 2000*, CYP3A enzymes are key players in the metabolism of two-thirds of commercially produced drugs.

DEX binds to and activates the glucocorticoid receptor (GR), a ligand-dependent receptor that belongs to the steroid nuclear receptor superfamily (Farrell and O'Keane 2016). The GR consists of three distinct regions. The N-terminal regions, with binding sites for transcriptional enhancement, the DNA binding

sites, with binding sites for dimerization, and the C-terminal region, with binding sites for hormones (e.g., glucocorticosteroids), coactivators, and heat shock proteins (Smoak and Cidlowski 2004).

Corticosteroids bind to the cytosolic GR which, upon binding, is translocated to the nucleus, where it dimerizes. It then either binds to the glucocorticoid response element (GRE) on the DNA of glucocorticoid-responsive genes to facilitate transcription or interacts with other transcription factors (Krieger et al. 2014). Interactions with other transcription factors like the estrogenic receptor (ER) or the thyroid hormone receptor, usually result in inhibitory effects rather than activation. Therefore, certain GR activating substances like DEX have anti-inflammatory properties or similar effects (Sonneveld et al. 2007). Figure 4 shows a schematic of the GR pathway.

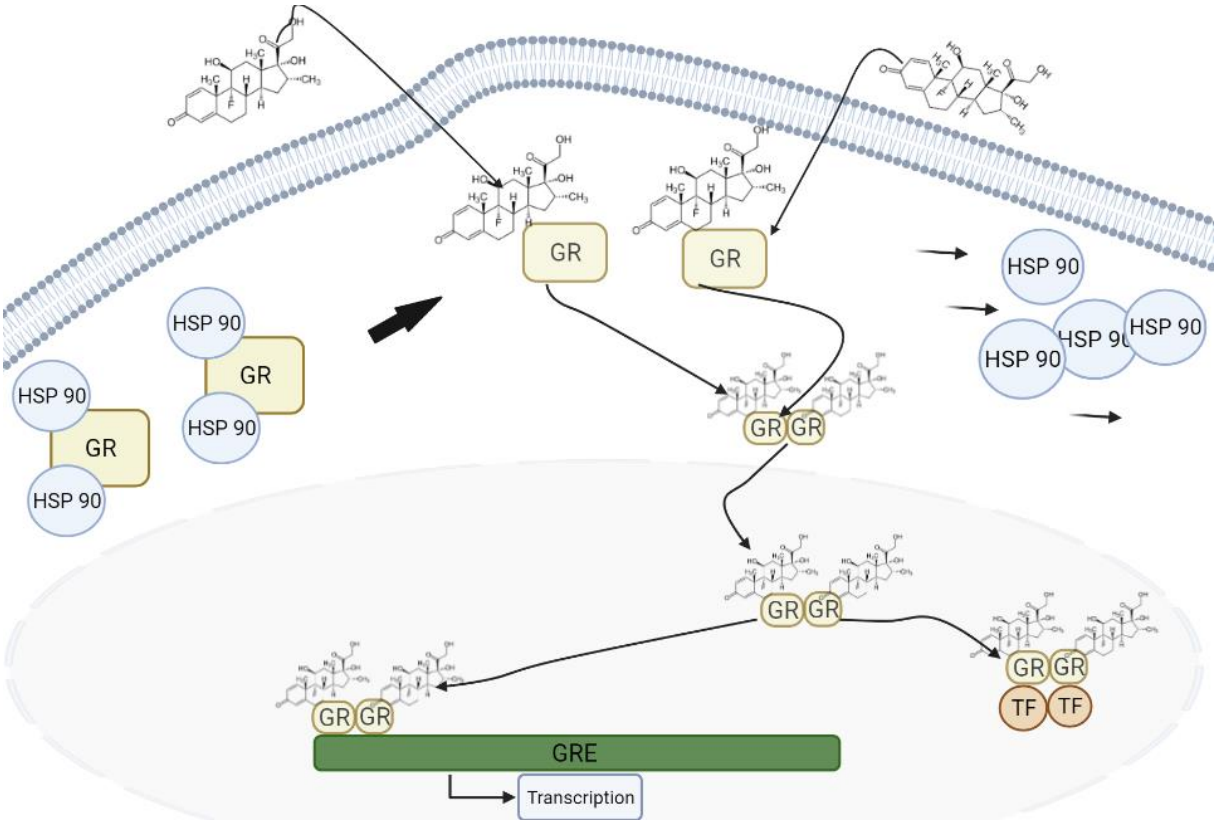

Figure 4: A simplified schematic of the GR pathway. DEX enters the cell through the cell membrane and binds to the dissociating GR complex. The bound GR dimerizes and transfers to the nucleus. Here the complex either binds to the GRE of a responsive gene to initiate transcription or to another transcription factor to initiate other cellular processes (Created with BioRender™).

1.5 Cytochrome P450

Cytochrome P450 (CYP) enzymes are membrane-bound haemoproteins that are key factors in the biotransformation and detoxification of xenobiotics. In Figure 5, the general CYP-mediated redox cycle is outlined. CYPs are also involved in various other metabolic processes and are crucial to maintaining homeostasis in the cell. CYP enzymes can be induced by numerous xenobiotics binding to different receptors. The increase in CYP abundancy upon exposure to a xenobiotic can be correlated to the relative toxicity of the molecule. This correlation is heavily used in toxicologic laboratory research for members of the CYP1A subfamily using the diagnostic Ethoxyresorufin-O-deetyhlase (EROD) assay (Petrulis et al. 2001).

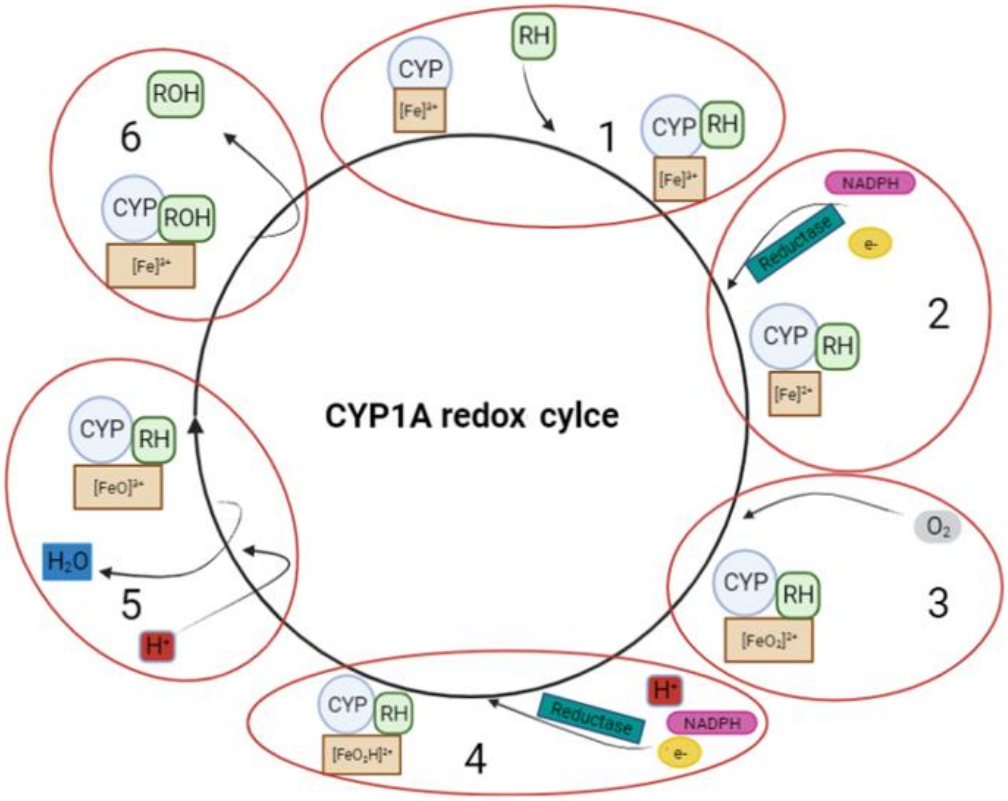

Figure 5: A simplified schematic of the CYP-mediated redox-cycle. (1): an organic compound binds to the CYP-$[Fe]^{3+}$ complex. (2): The newly formed complex gets reduced mediated by the CYP-reductase enzyme, a donor electron, and the co-factor NADPH. (3): Oxygen binds to the complex. After this step, there is the potential of the formation of a reactive oxygen species (ROS; Superoxide O_2^-)! (4): The complex gets reduced again as in (2) but this time also a proton is added. After this step, another ROS could form (Hydrogen peroxide H_2O_2)! (5): After the addition of another proton, water gets cleaved off from the complex. (6): A hydroxide is formed, and the oxidized organic compound leaves the cycle (Created with BioRender™).

The expression of CYPs is prone to be influenced by drug-drug/xenobiotic interaction which can activate or inhibit transcription. This can have fatal consequences leading to unexpected outcomes of medical treatment and therapeutical failure. Also, the biotransformation of xenobiotics can cause toxicity in cells. In the process of bioactivation, the CYP enzymes can facilitate the conversion of xenobiotic molecules

to more reactive products that can undergo damaging reactions with proteins and DNA. Furthermore, biotransformation reactions can lead to the formation of oxygenated by-products that can cause oxidative damage to the cells (Guengerich 2008; Jana and Paliwal 2007; Manikandan and Nagini 2018).

1.6 AhR-GR Receptor Crosstalk

Crosstalk between the AhR and the GR has been suspected for many years and several scientists have published papers on that matter. By testing DEX in mixtures with different AhR agonists as 2,3,7,8-tetrachlorodibenzo-p-dioxin (TCDD) or 3-methylcholanthrene (3-MC), it quickly became apparent, that endpoints such as protein and mRNA levels changed compared to the effects single compounds have.

Dvořák et al. (2008) investigated the effect of TCDD + DEX in HepG2 cells and concluded that there is cross-induction of the XRE and the GRE. While XRE-dependent expression decreased, GRE-dependent expression was augmented by exposure to mixture. They also found that while after single substance exposure (both DEX and TCDD), the AhR mRNA levels were lower compared to untreated cells, this inhibitory effect was reverted after combined treatment of TCDD + DEX. Same was true for GR α levels (compared to exposure to DEX) (Dvořák et al. 2008).

Wang et al. (2009) found there to be down-regulation of AhR agonist-mediated CYP1A induction in human ovarian and liver cells after treatment with DEX + BaP, thus confirming the findings from Dvořák et al. Wang et al. further concluded that the AhR and the GR, both must be activated for a receptor cross-reaction to occur (Wang et al. 2009).

Monostory et al. (2004) did not see a decrease in AhR-dependent transcriptional activity (CYP1A mRNA) after exposure of human hepatocytes to 3-MC + DEX. However, they suggest that the 3-MC concentration may have been high enough so that the diminishing effect of DEX was negligible. They; however, detected strong down-regulation of CYP1A at the protein level. To compare the effects of 3-MC + DEX, they also conducted experiments on rat hepatocytes which revealed that, in contrast to humans, the CYP1A activity is highly induced by DEX (Monostory et al. 2005).

Bielefeld et al. (2008), confirmed the potentiation effect of DEX in rodents when testing TCDD + DEX on mouse hepatoma cells (Hepa-1). They found there to be an increase in AhR mRNA, AhR protein level and TCDD binding capacity after mixture exposure. As the response was blocked, through the addition of a GR antagonist (RU-486), it was confirmed that the activation of the GR receptor was the reason for the potentiating effect (Bielefeld et al. 2008).

These so far seen species specific effects were also observed by Sonneveld et al. (2007), who detected upregulation of AhR signalling upon exposure to a mixture of TCDD + DEX in rats but not in humans. They were also able to show that the enhancing effect of DEX is dependent on the additional synthesis of the AhR protein (Bielefeld et al. 2008; Sonneveld et al. 2007).

Celander et al. (1996), tested the mixture toxicity of DEX + TCDD in a fish cell line (PLHC-1) and showed potentiation of CYP1A induction after mixture treatment, compared to TCDD alone. The potentiating effect was higher after 48 h of exposure than after 24 h and peaked at a TCDD concentration of 1 nM. As the addition of RU-486 reduced the potentiating effect of DEX, Celander et al. suggest that the potentiation is, at least to a certain extent, dependent on GR activity (Celander et al. 1996).

2. Materials and Methods

2.1 Materials

2.1.1 Cell Line

The model organism of choice for the experiments described in this thesis, is the *Poeciliopsis lucida* hepatocellular carcinoma cell line I (PHLC-I, CRL-2406 ™). The cell line was derived from an adult female topminnow *Poeciliopsis lucida*, endemic to the Sonoran Desert (US). It is designed so several differentiated hepatocellular functions are maintained, and it is optimized for *in vitro* research. A special focus has been placed so the cell line maintains a stable cytochrome P450 activity. The cell line is commonly used to investigate stressors such as heavy metals, and for cytotoxicity assays (ATCC 2022; Ibarra et al. 2021).

2.1.2 PLHC-I Medium

To prepare 1 L of PHLC-I medium, Gibco® Minimum Essential Medium (MEM) powder is dissolved in 850 mL of Milli-Q H_2O and stirred for 10 min. 5.96 g of HEPES and 2.2 g of $NaHCO_3$ are added and stirred for 10 min (the colour of the solution turns from yellow to red). The pH is adjusted to 7.0-7.1 using NaOH. The final volume is reached by the addition of 150 mL of Milli-Q water. The solution is filtered through a 0.2 μm sterile filter into one or more autoclaved flasks. Fetal Bovine Serum (FBS) is added (10 % of the final volume). The bottle is stored at 4 °C and covered in aluminium foil to protect from light as the media contains light sensitive chemicals such as indoles.

2.1.3 Culture plates

For our experiments, sterile, flat bottom, non-pyrogenic, polystyrene cell culture plates were used. We predominantly used 6-well (3516, Costar ®) and 48-well (3548, Costar ®) plates.

2.1.4 EROD

REAGENTS

7-Ethoxyresorufin

2 µM of 7-ethoxyresorufin in Sodium phosphate Buffer (pH 8.0) is prepared utilizing absorbance measurement. The solution is prepared so the absorbance at 482 nm yields 0.06 which corresponds to a concentration of 2.67 µM 7-ethoxyresorufin.

Fluorescamine

A 1.08 mM solution of fluorescamine is prepared by dissolving 3 mg of fluorescamine in 10 mL of acetonitrile.

Phosphate Buffered Saline (PBS, Ca^{2+}/Mg^{2+} free)

PBS [1 L] is prepared by the addition of 8 g NaCl (~137 mM), 0.2 g KCl (~2.7 mM), 3.56 g $Na_2HPO_4x12H_2O$ (~10 mM) and 0.24 g KH_2PO_4 (~1.8 mM). The pH is adjusted to 7.3-7.4 and the solution is autoclaved and stored at room-temperature.

Ethylenediaminetetraacetic acid-PBS (EDTA-PBS) solution

EDTA-PBS [1 L] is prepared by the addition of 0.20 g of EDTA ($C_{10}H_{14}N_2O_8Na_2$ x $2H_2O$) to 1 L of PBS.

50 mM Sodium Phosphate Buffer

The Sodium Phosphate Buffer [250 mL, 50mM] is prepared by the addition of 11.65 mL Na_2HPO_4 (1 M) and 0.85 mL NaH_2PO_4 (1 M) to 237.5 mL of Milli-Q H_2O. The pH is adjusted to 8 and the buffer is autoclaved and stored at room temperature.

2.2 Methods

2.2.1 Cell Culture

The PHLC-I cell line was cultured at 30 °C in 75 cm^2, non-vented flasks with tight screw caps.

Sub-culturing from a 75 cm^2 flask

The media from the culture flask is removed by vacuum suction without physically disrupting the cells. The cells are rinsed with 5 mL of room temperature warm trypsin-EDTA (2x, 0.05 (v/v)). The cap of the flask is exchanged, and the cells are incubated at room-temperature for 1-5 min. The cells are dislodged, and 10 mL of growth medium are added. The cells are separated by pipetting up and down. An adequate number of cells and an appropriate amount of medium are added to a new flask (final volume 20 mL). The flask is gently mixed and moved to the incubator.

Plating of PHLC-I cells

After dislodging the cells as the described earlier, the cells are resuspended in 20 mL. An aliquot of well-mixed cells is taken and counted utilizing a hemacytometer. The number of cells required for the experiment is calculated. The cells, diluted adequately with growth medium, are gently stirred in a beaker. The homogenized suspension is plated (500 µL per well for 48–well plates, 2 mL for 6–well plates). The plate is sealed with parafilm and placed in the humidified incubator at 30 ˚C. The medium is changed after 24 h.

2.2.2 EROD-assay

Theory

Induction of CYP1A enzyme activity is a common biomarker to assess exposure to aromatic hydrocarbons in human cells but also in fish cells. In our study, we focus on the CYP1A enzyme which is known to be induced by PAHs and similarly behaving aromatic hydrocarbons and is the key driver in biotransformation process of these compounds. Hence the abundance of CYP1A directly correlates to the abundance of the AhR agonist.

In the EROD assay one makes use of an associate reaction, 7-ethoxyresorufin to resorufin, which is catalysed by the CYP1A enzyme. Also here, the amount of resorufin produced, directly correlates to the amount of free CYP1A enzymes present in the cell. The natural fluorescence of the reaction product resorufin, makes a quantification possible. Both 7-ethoxyresorufin and the xenobiotics compete for the same receptor sites. Hence, the EROD activity does not reach a "saturation plateau" but declines over time (Petrulis et al. 2001).

Assay procedure

After taking the culture plate out of the incubator the medium is carefully removed by vacuum suction. The wells are rinsed once with 500 µL of PBS. After aspirating off the PBS, 200 µL of 7-ethoxyresorufin are added to each well. The plate is subsequently moved to the fluorometer (Victor ™ 1420 Multilabel Counter, excitation wavelength: 540 nm, emission wavelength: 580 nm) for analysis.

Bovine Serum Albumin (BSA) Standard Plate

The BSA standard plate is prepared by serial dilution (0.0625, 0.125, 0.25, 0.5, 1 mg mL^{-1}). The solutions are added in duplicates to a 48-well plate and measured in the fluorometer (excitation wavelength: 365 nm, emission wavelength.: 470 nm).

Resorufin Standard Plate

A dilution series of resorufin in a range from 6.25 pmol to 200 pmol (6 concentrations) is made in a 48-well plate. 100 µL of fluorescamine solution are added to each well. The plate is wrapped in aluminium foil and incubated on a shaking platform at room-temperature (for 10 min) before measuring the total cellular protein content in the fluorometer.

Calculations

The results of the BSA measurement, are plotted to create a quadric standard curve to determine the protein concentration in the PLHC-1 samples. In contrast to the BSA standard curve, the resorufin standard curve is linearly fitted.

To derive the EROD activity, the fluorometer measures the fluorescence 10 times in each well. The resulting values are plotted against the runtime and linearly fitted. The slope is divided by the slope of the resorufin standard curve to yield the EROD activity [pmol min^{-1}]. By dividing through the amount of protein the Specific EROD activity [pmol resorufin $protein^{-1}$ min^{-1}] is determined.

2.2.3 Quantitative PCR (qPCR)

Theory

In contrast to conventional PCR, in quantitative PCR or real-time PCR, the final product is not determined by an end-point analysis but by quantification after each cycle throughout the mRNA synthesis process. By using fluorescent DNA dyes or sequence-specific probes, the product can be determined quantitatively. Compared to conventional PCR, this method saves time, and laboratory work and no analysis by DNA gel electrophoresis is required (Bio-Rad Laboratories 2022).

Cell lysis, RNA extraction, and purification were performed using the Qiagen RNeasy® Mini Kit and the protocol provided.

Lysis of PLHC-I cells

The cell media is removed by vacuum suction and the cells are rinsed once with PBS. After aspirating off the PBS, 350 µL of RLT Buffer (1% β-mercaptoethanol) is added to each well. By scratching the bottom surface with a filter pipette tip, the cells are detached from the wells. The suspension is homogenized by pipetting up and down and transferred to an Eppendorf tube (1.5 mL). The cell lysate is stored at -80 °C or kept on ice for subsequent RNA extraction.

RNA Extraction and Purification

To avoid degradation, not more than 12 samples are processed at a time. The cell lysate (thawed) is vortexed and briefly spun down. The suspension is then added to the homogenisation column and centrifuged (2 min, max. speed). The flowthrough is then transferred to the gDNA elimination column and centrifuged again (30 sec., max. speed). Then, the flowthrough is added to the RNeasy spin column

together with 350 µL of ethanol (70%). The mixture is homogenized by pipetting up and down and centrifuged (15 sec., max. speed). The flowthrough is discarded, and the tube is dabbed on a tissue for more efficient waste removal. 700 µL of washing buffer 1 are added to the same column which is centrifuged for 15 sec. (max. speed). This procedure is repeated twice with 500 µL of the RPE buffer (centrifuged 15 sec. 1^{st}, 2 min 2^{nd}; max. speed). Then the RNeasy spin column is placed in a new collection tube (1.5 mL) and 30 µL of RNAse-free water is added directly onto the membrane. To elute, the column is centrifuged for 1 min. (max. speed). The elution is transferred to a new 1.5 mL Eppendorf tube. The total RNA concentration is determined by NanoDrop™ measurement. The RNA samples are alternatively stored at -80°C or kept on ice for subsequent cDNA synthesis.

Synthesis of cDNA

The thawed samples are briefly spun down, then vortexed and spun down again (S-V-S) before being put back on ice. The master-mixture is prepared according to the number of samples and subsequently homogenized (S-V-S). The cDNA reaction mixture is prepared in RNAse-free Eppendorf tubes (0.2 mL) according to the concentration of the RNA. Two control samples are prepared (1^{st} without reverse transcriptase, 2^{nd} without RNA). The samples are homogenized (S-V-S) and loaded into the machine.

PCR plate preparation and qPCR measurement

The cDNA is homogenized (S-V-S) and diluted with RNAse-free water to 2.5 ng μL^{-1} in new Eppendorf tubes. The reaction mixture (RM) containing the primers and the SYBR™ green dye, is prepared and homogenized (S-V-S). To prepare the PCR plate, a droplet of the sample (4 µL) is added to the wall of one side of the well. Additionally, a control sample containing water is added. Samples and controls are added in triplicates. After adding all the sample droplets, the plate is carefully rotated, and the RM (6 µL) is added in the same manner on the other side of the well. Then the plate is thoroughly sealed to avoid evaporation and spillage and subsequently vortexed and centrifuged (2 min., 1000 g). Finally, the plate is moved to the PCR machine and analysed.

Calculations

For each sample that is measured for CYP1A mRNA, a separate qPCR run is performed to measure the 18 S housekeeping gene. The average cycle quantification value (Cq-value) including measurements for each biological replicate is derived. The average value for 18 S is subtracted from the average value for CYP1A. The result value (dCq), referred to as "relative mRNA level" of the sample is plotted as $(2^{-Cq}) * 10^6$.

2.2.4 Gas Chromatography – Mass Spectrometry (GC-MS)

Theory

The detection principle in GC is based on the movement of a gaseous compound transported by a mobile phase along a stationary phase. To be able to measure a compound in GC, it must be thermically stable and volatile. MS is a type of detection system where compounds are ionized and separated by means of electric or magnetic fields. A number of fragments for each sample with, the respective mass in a mass to charge ratio (m/z), is the output of the analysis. With GC-MS it is possible to create a total ion current chromatogram (TIC) which depicts the abundance of each ion in the sample represented as a peak with the integrated area below corresponding to the relative abundance of the respective ion. To identify a peak of interest a scan with a positive control must be conducted to evaluate the retention time of the respective ion (Honour 2006).

Assay

The cell medium is aspirated off and the cells are rinsed with 2 mL of PBS once. After aspirating off the PBS, 200 µL of trypsin (25%) are added to each well to detach the cells from the surface of the well. After 2 min, the suspension is transferred to an Eppendorf tube (1.5 mL). Then 200 µL of acetone are added to each tube and the suspension is homogenized (spin-vortex-spin, S-V-S). Then 200 µL of heptane are added to each sample and the suspension is mixed again (S-V-S). Now, the samples are sonicated in a sonication bath for 10 min. Afterwards, the upper, organic layer of each sample is transferred to a glass vial.

The samples are measured in the GC-MS machine in SIM mode with splitless injection.

The machine utilized, is a GC system (Agilent Technologies, 7890A GC system) with a Mass selective detector (Agilent Technologies, 5975C inert XL/EI/CI MSD + Triple-Axis detector), equipped with a Autosampler (Agilent Technologies 7693).

2.2.5 Statistical analysis

For the statistical analysis of the results derived from EROD assays, the Wilcoxon rank-sum test was performed. A p-value < 0.05 was considered significant.

2.2.6 Software

This thesis was written in Microsoft® Word. The data treatment was performed using Microsoft® Excel and R® Studio. The figures displayed here were created using R® Studio and BioRender™.

3. Results

3.1 EROD assay

To make the data presented comparable, even between different experiments, all values have been normalized. As the vehicle control, DMSO does not activate the AhR signalling and therefore does not induce CYP1A which would lead to detection of EROD (CYP1A) activity, the values received are not suitable for normalization as they are often negative. Therefore, the lowest concentration of the "positive control" is used as a control value instead.

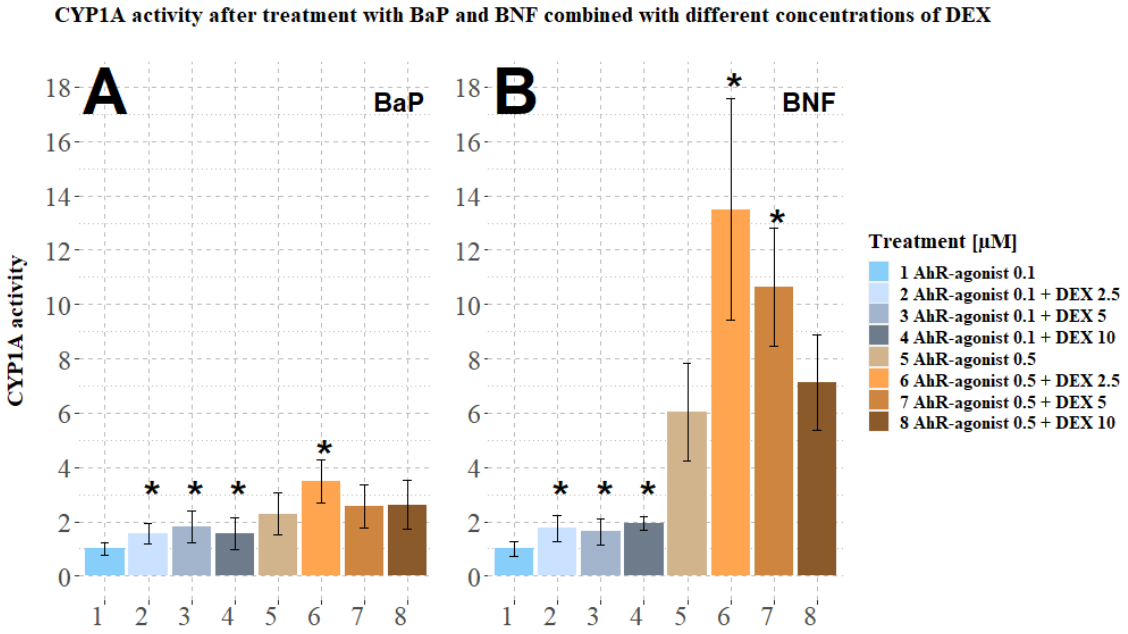

Figure 6: Mean specific EROD activity (24 h exposure) normalized to the activity of the sample after treatment to 0.1 µM of BaP (A) and BNF (B) respectively. The data points in "A" were generated from the arithmetic mean of 16 values from four repetitions of the same experiments (Except for bar "1", BaP 0.1 µM with 12 values). For "B", two experiments were conducted using 8 values per treatment to derive the arithmetic mean. The error bars show the standard deviation of the datasets. The * indicates that the dataset is significantly different from the respective control ($p < 0.05$).

Figure 6 A shows an average activity for BaP 0.5 µM (Bar 5) which is ~ 2.3-fold of BaP 0.1 µM (Bar 1), wherein B, the activity of BNF 0.5 µM (Bar 5), is ~6 times higher than BNF 0.1 µM (Bar 1). In contrast to the mixture effect seen with BaP (Figure 6 A), the difference in average EROD activity seen in B is significantly higher for mixtures with higher BNF concentrations. Figure 6 A suggests that for mixtures with BaP 0.5 µM, the mixture effect is greatest at lower DEX concentration, while the two mixtures with higher DEX concentration show similar values. This observation appears to be in line with what can be observed for BNF in Figure 6 B. However, after statistical analysis, we conclude that in contrast to A, bar 6 is not significantly different from bar 7. Bar 8, however, is significantly lower than bars 6 & 7 (Table A1, 4-6).

Not displayed in either of the graphs is the activity resulting from the treatment of the cells with the negative control (DMSO) and DEX (5 µM, 10 µM) individually, as neither of them suggests a significant induction of CYP1A enzyme activity.

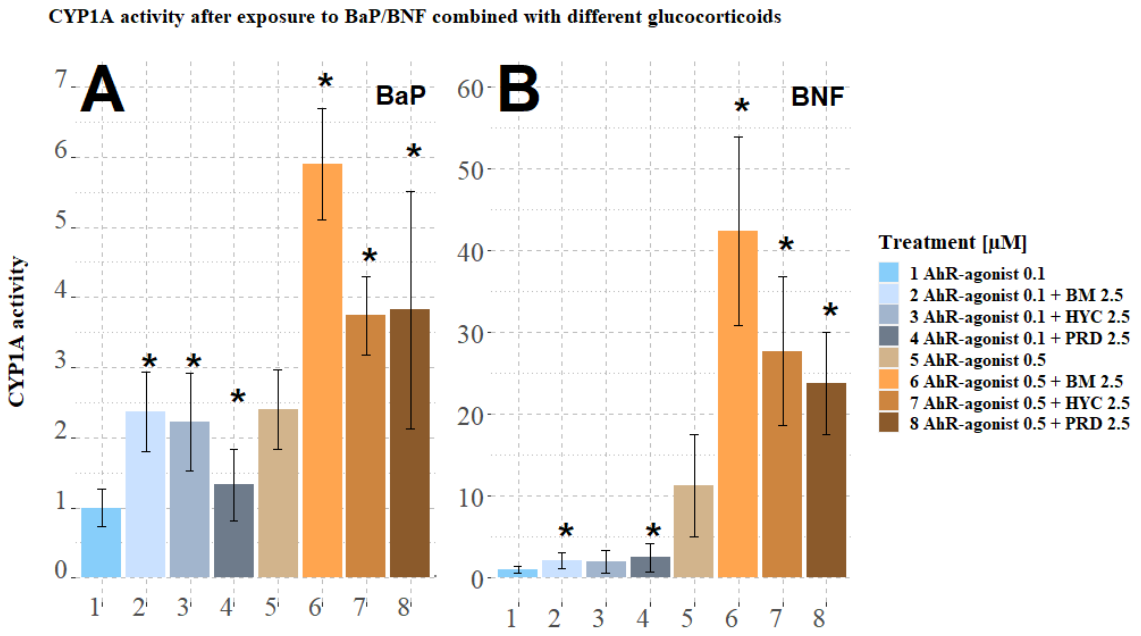

Figure 7: Mean specific EROD activity (24 h exposure) normalized to the activity of the sample after treatment to 0.1 µM of BaP (A) and BNF (B) respectively. The data points in "A" were generated from the arithmetic mean of 16 values from four repetitions of the same experiments. For "B", three experiments were conducted using 12 values per treatment to derive the arithmetic mean. The error bars show the standard deviation of the datasets. NOTE: A & B have different scales on the y-axis. The * indicates that the dataset is significantly different from the respective control ($p < 0.05$).

The difference in activity between the two concentrations for BaP tested (0.1, 0.5 µM), appears greater in Figure 7 A (BaP 0.5 µM 2.4-fold of BaP 0.1 µM) than in Figure 6 A (2.29-fold). Notably, the concentration-dependent difference in activity for cells treated with BNF only (B, 0.1 and 0.5 µM) appears much more significant than seen in previous results (Figure 6 B).

In terms of mixture toxicity, Figure 7 A shows similar values for BM and HYC (with BaP 0.1 µM), but significantly lower mean EROD activity when PRD is in the mix. This is not true with BNF as AhR agonist (Figure 7 B), where the mixtures with different glucocorticoids, all result in similar EROD activity.

With higher BaP concentration in the mixture (A), we see that BM causes the highest potentiation (~ 2.5-fold) out of the three glucocorticoids, which is still lower than seen for BNF as an AhR agonist (~ 4.0-fold, B). In A, the other two glucocorticoids cause similar, lower potentiation (~ 1.5-fold), whereas BaP + PRD; however, has a much higher standard deviation. In B however, a regression can be observed (BM > HYC > PRD); however, the difference between 7 & 8, turns out not to be statistically significant (Table B1, 12).

Not displayed in either of the graphs is the activity resulting from the treatment of the cells with the negative vehicle control (DMSO) and the glucocorticoids (2.5 µM) individually, as neither of them suggests a significant induction of CYP1A.

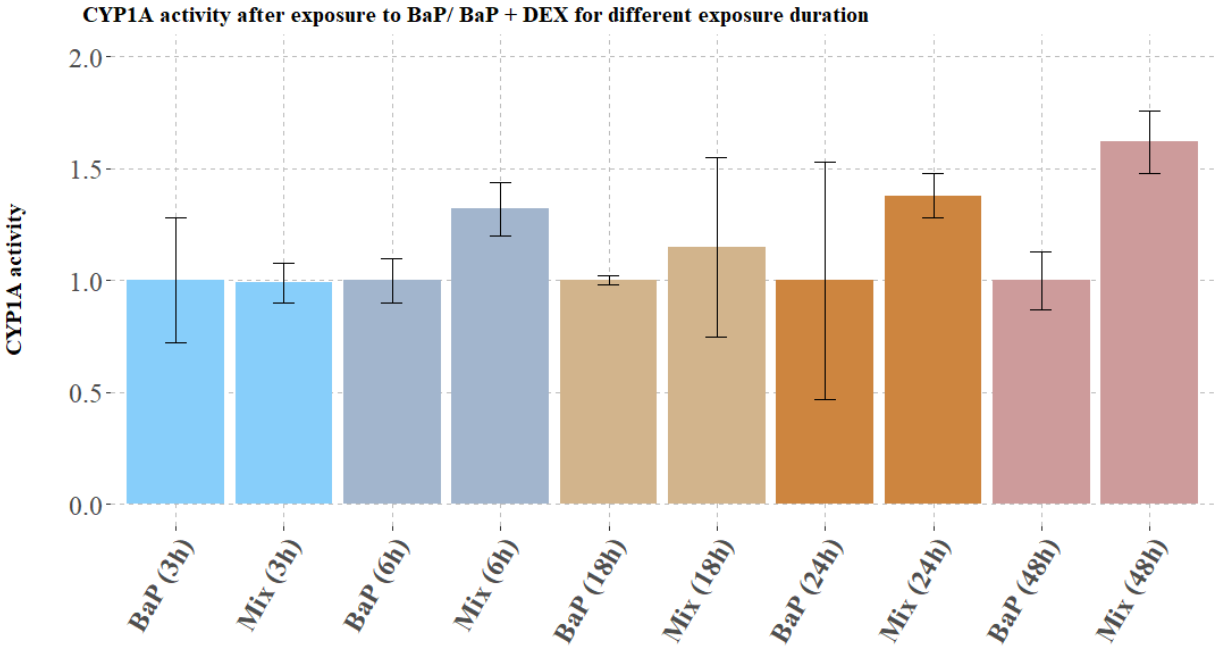

Figure 8: Mean specific EROD activity of cells treated with either BaP (0.1 µM) alone or in a mixture with DEX ("Mix" = 0.1 µM BaP + 2.5 µM DEX) after different exposure times. The data is normalized for each exposure time (BaP 0.1 µM set to 1). The data points were generated from the average data from four observations of the same experiments (except for 4 with three observations). The error bars indicated the standard deviation. Not displayed are the results for the vehicle control samples, the activity after exposure to DEX alone, and the activity after 10 min of exposure time to BaP and BaP + DEX. Due to the small number of replicates for each dataset, no statistical analysis would have been feasible and was therefore not performed.

Figure 8 shows the difference in Mean specific EROD activity between cells treated with BaP 0.1 µM and in a mixture with DEX 2.5 µM, for 5 different exposure times. The results reveal a general increase in mixture effect with increasing exposure time. While after an exposure time of 3 h (1 & 2), the resulting EROD activity is virtually identical (Table C1, 5) for both BaP and Mix, the potentiation after mixture exposure increases over time, reaching a maximum of a 1.6–fold difference after 48 h of exposure (9 & 10). Interestingly, bars 3 & 4 (6 h exposure) appear to differ to a greater extent than bars 5 & 6 at a higher exposure time. It must be considered; however, that Figure 8 shows data resulting from a small set of replicates with a high standard deviation (as seen e.g., bar 7). Also, previous results with a higher number of replicates and lower standard deviation, show a tendency that slightly deviates from what is displayed in Figure 8. In Figure 6 A, we see that BaP 0.1 µM + DEX 2.5 µM has a ~ 2-fold activity after 24 h exposure compared to BaP 0.1 µM alone were for Figure 5 only shows a ~ 1.4-fold increase for the same exposure time (Figure 8, 7 & 8). The activity after a 10 min exposure of the cells to BaP and the

mixture respectively, is not displayed in Figure 5. The activity; however, does not differ from the activity seen for the solvent (Table C1, 1-4).

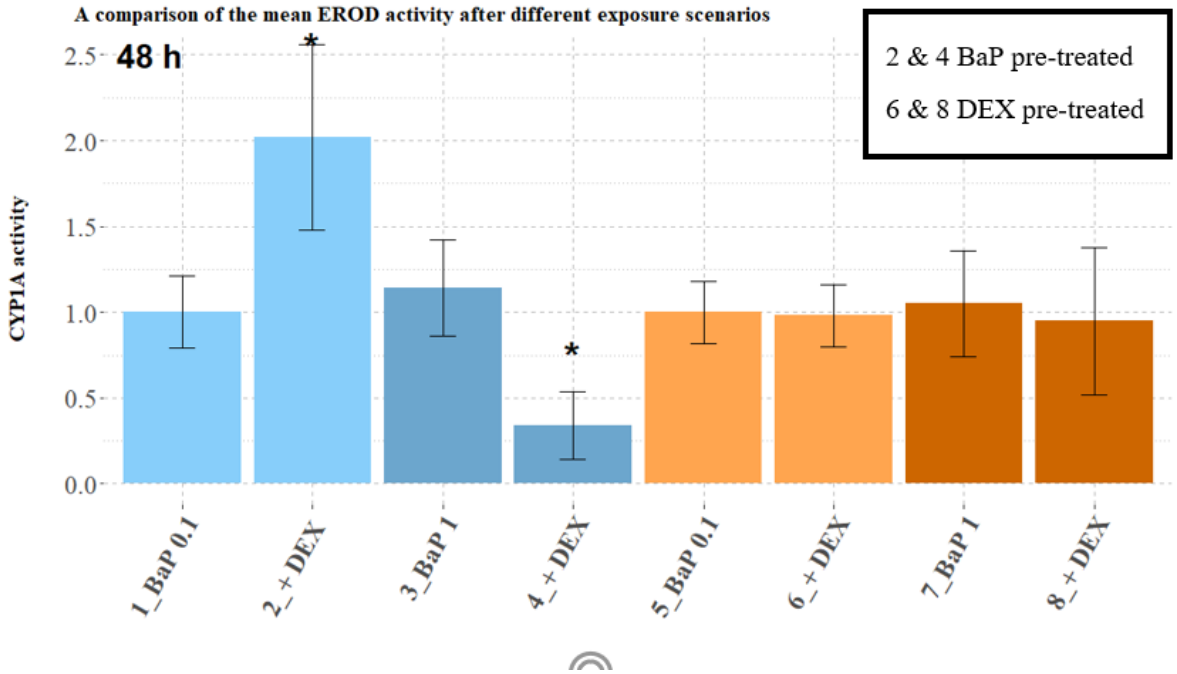

Figure 9: Mean specific EROD activity of cells treated with BaP (0.1, 1 µM) or BaP + DEX (10 µM) after different exposure times. In mixtures on the left side of the graph (2 & 4) BaP was added first with DEX being added 24 h later. The overall exposure time was 48 h. In the mixtures on the right side (6 & 8), the opposite procedure was executed. For treatment with BaP alone (1, 3, 5, 7), the exposure time was 48 h. For each exposure type, the data is normalized setting BaP 0.1 to 1. The bars were each generated from an average of 8 replicates. The error bars indicated the standard deviation. The * indicates that the dataset is significantly different from the respective control ($p < 0.05$).

In Figure 9, depicts the results from an experiment utilizing different pre-exposure scenarios. While on the left the mixtures (2 & 4) were pre-exposed with BaP (24 h), the mixtures (6 & 8) on the right were pre-exposed to DEX (24 h) before adding the other substance respectively. The overall exposure time was 48 h.

When comparing the mixture effect for the lower BaP concentration (0.1 µM), we notice a potentiation in EROD activity on the left side (1 & 2) while no difference can be observed on the right side (1 & 6; $p > 0.05$, Table D1, 2 & 5). This suggests that pre-exposure with BaP/ delayed addition of DEX has a greater effect on the EROD activity and therefore, CYP1A induction.

After comparing the mixture effect for the higher BaP concentration (1 µM); however, we observe a negative mixture effect after BaP pre-exposure (3 & 4), whilst there is once again no significant difference between the treatments on the right side (7 & 8; $p > 0.05$, Table D1, 6).

Figure 9 further indicates a dose-response for BaP, where treatment with a higher BaP (1 µM) concentration leads to a greater EROD activity (1 & 3). However, due to the high variability in the datasets, no significant statistical difference can be observed (Table D1, 1 & 4).

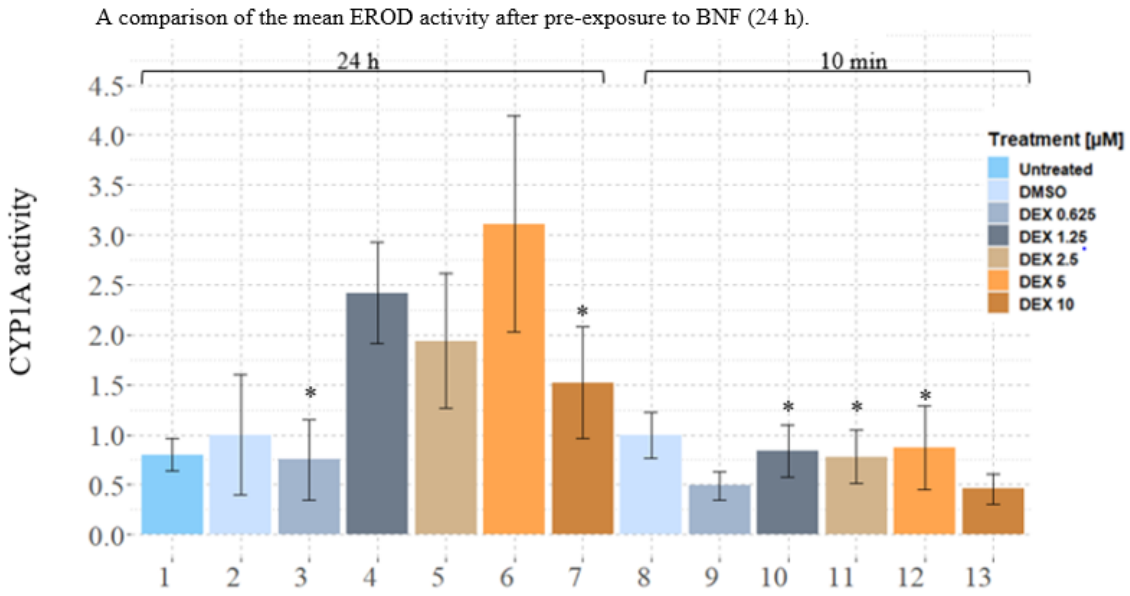

Figure 10: Mean specific EROD activity of cells after exposure to different DEX concentrations after BNF (0.1 µM) pre-exposure (24 h). Two different exposure scenarios are displayed. Bars 1-7 show the activity after 24 h of exposure of the pre-treated cells. While for bars 8-13 the exposure time was only 10 min. For both scenarios the data is normalized setting the negative vehicle control DMSO to 1. The bars were generated from an average of 4 replicates each. The error bars indicate the standard deviation.

Figure 10 shows the EROD activity after short (10 min) direct and long (24 h) exposure of BNF (0.1 µM, 24 h)) pre-treated cells, to different DEX concentrations. The Figure clearly illustrates that after 24 h a potentiation takes place (except for bar 3, DEX 0.625 µM), while after a short exposure time of 10 min, appears similar or even lower than the control.

Bars 3 & 7 do not differ significantly from the vehicle control, Bar 2 (Table E1, 2 & 3) which is also true for bars 10-12, which do not differ from bar 8 respectively (Table E1, 4-6).

The data further suggests a concentration dependency for DEX, as after 24 h the potentiation increases significantly with increasing DEX concentration. The trend differs slightly from results after 24 h combined mixture exposure of untreated cells, as seen earlier (Figure 6), where a concentration dependent decrease in potentiation can be observed after a peak at DEX 2.5 µM. However, here, also the lower number of replicates and the high variability in Figure 7 must be considered.

The DEX concentrations 1.25, 2.5 and 5 µM, result in higher EROD activity after both exposure scenarios.

3.2 qPCR analysis

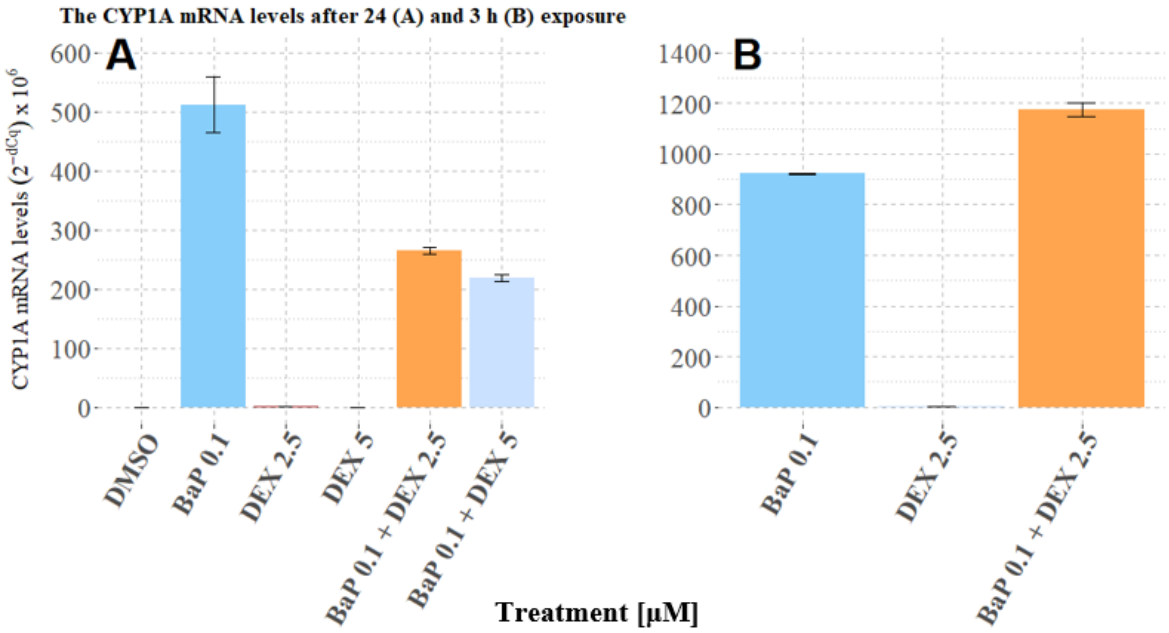

Figure 11: An illustration of the CYP1A mRNA level after different treatments of PHLC-I cells. A: 24 h treatment, 3 replicates per bar; B: 3 h treatment; 2 replicates per bar.

Figure 11 shows the relative CYP1A mRNA level after the exposure of the cells to different treatments for different time. In A, we see that DMSO and DEX (2.5 and 5 µM) do not cause any notable expression of CYP1A mRNA compared to the other treatments. This is true for the exposure to the chemicals for 24 h (A) but also after 3 h of exposure (B).

After 24 h of exposure, we see that treatment with BaP (0.1 µM) alone, results in much higher mRNA expression as compared to the mixture treatment. Figure 11 A also suggests that a higher concentration of DEX in the mixture, further lowers the mRNA production after 24 h. In Figure 11 B, after an exposure time of 3 h, we see a contrary picture where the mixture treatment causes a higher CYP1A mRNA level compared to BaP alone (~1.3-fold).

3.3 GC-MS analysis

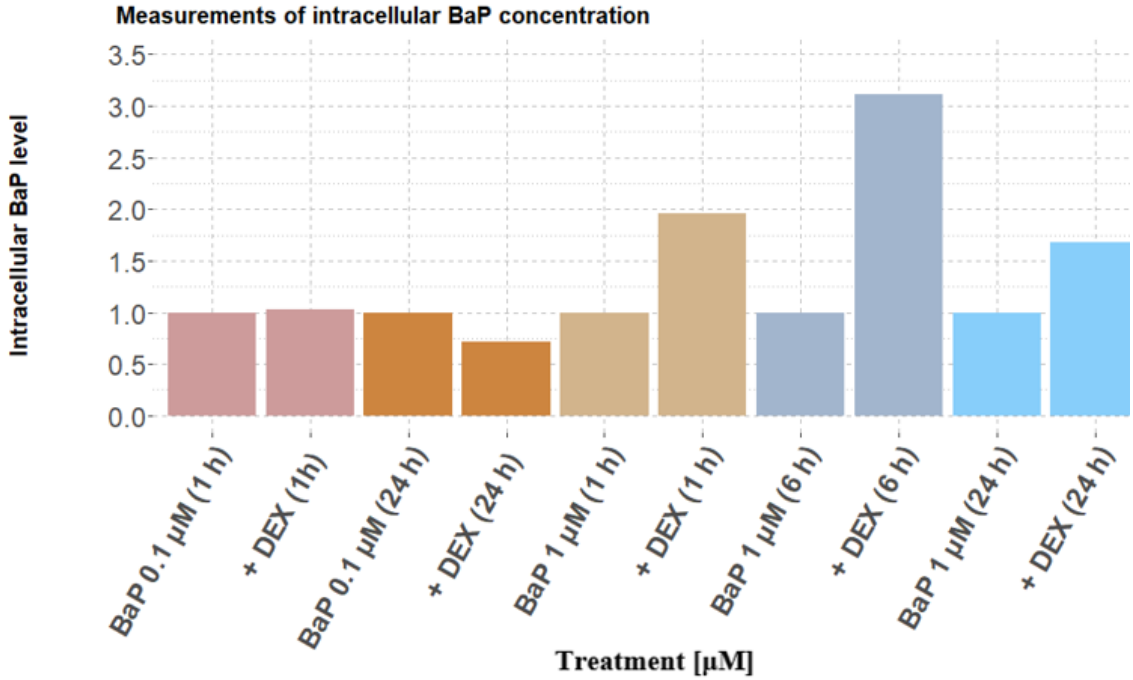

Figure 12: An illustration of the intracellular BaP levels after treatment with BaP or BaP + DEX for different concentrations and exposure durations. The BaP levels are determined after GC-MS measurement and expressed as an integration of the peak area which corresponds to BaP as identified after a nalysis of a positive control sample. The data presented here is normalized and expresses the fold of the BaP level after mixture treatment for each concentration and exposure time, relative to the BaP control. The DEX concentration for all treatments was 2.5 µM. The data shows the results for one single sample per bar.

Figure 12 shows the results from the GC-MS measurement of different cell samples after different treatments and different exposure times. As we see on the left side of the graph, there is little difference in intracellular BaP abundancy after treatment with BaP 0.1 µM or BaP 0.1 µM + DEX 2.5 µM for 1 h. After a longer exposure of 24 h to the same treatments, we see lower BaP levels after mixture treatment. With increasing BaP concentration, however, our data indicates higher BaP levels after mixture treatment, for every exposure time tested. Our data suggest that the difference in response peaks somewhere between 1 h and 24 h as the response after 6 h is significantly higher than for the control.

4. Discussion

In this study, the changes in CYP1A induction in PLHC-I cells were assessed, based on exposure to BaP and DEX independently, as well as in mixtures of different composition and concentration. Moreover, changes in CYP1A induction, based on different exposure scenarios, as variations in exposure time and experiments on pre-exposed cells, were investigated. To place our findings into perspective, additional AhR agonists and GR agonists were tested analogously.

4.1 Dose-Response findings of DEX

DMSO and DEX were tested in various EROD experiments. As Table 5 outlines, the derived data strongly suggests, that there is no significant difference in EROD activity (and thus, CYP1A induction) detected in cells treated with DMSO and cells treated with DEX. This tendency is also true for the experiments conducted to investigate the activity after different exposure times (0.16, 3, 6, 18, 24, 48 h) and experiments involving different DEX concentrations (2.5, 5, 10 µM).

Therefore, our findings indicate that DEX does not possess the potential to activate the AhR in PHLC-I cells, for the concentrations and exposure times tested. Celander et al 1996, produced similar results, when comparing data after 48 h exposure of PHLC-I cells to DMSO and DEX (10 µM) from 10 experiments (8 replicates each). Although Celander et al. state that half of the experiments yielded a slightly higher EROD activity for cells treated with DEX, they point out that the values measured are close to the detection limit of the assay and are negligible compared to the activity measured after treatment with AhR-agonist TCDD (Celander et al. 1996). Previous studies showed that the effect DEX has on hepatic cells differs not only between mammals and fish but even within fish species (Burkina et al. 2015). As there is limited data on DEX-exposure of PHLC-I and other fish cells, is it difficult, at this stage, to put our findings into perspective.

4.2 Dose-Response findings of DEX in a mixture

To get an insight into whether and how the concentration of DEX affects CYP1A induction in cells treated with DEX + an AhR agonist, experiments were carried out testing different DEX concentrations in combination with either BaP or BNF.

The results, as illustrated in Figure 6, reveal that in combination with BNF, a lower DEX concentration yields a higher EROD activity (2.5 > 5 > 10 µM DEX). In combination with BaP, the lowest DEX concentration tested (2.5 µM) also results in the highest potentiation (Figure 6 A). In contrast to the data involving BNF, however, the activity does not strictly regress with increasing DEX concentration, as BaP + DEX 5 µM and BaP + DEX 10 µM appear to show similar EROD activity. It must also be

considered that the data for BNF + DEX mixtures (Figure 6 B) shows a higher standard deviation and represents a lower number of replicates than the data shown in Figure 6 A.

In mixtures with lower AhR-concentration, the trend for this concentration range does not hold true. Although slight variations in activity can be observed in Figures 6, statistical analysis shows that almost none of the displayed datasets in question are significantly different from the others (Table 5, 1-39). A few comparisons that turned out to be statistically different, show a higher mean average EROD activity after DMSO treatment (Table 5, 26-34).

Celander et al. 1996, tested the concentration dependency of DEX in mixtures with TCDD (24 h exposure, PLHC-I cells) and observed the highest peak of CYP1A induction at a DEX concentration of 0.01 µM (Celander et al. 1996).

As the exact interaction mechanism between BaP and DEX remains unclear, one can only hypothesize on the dose-response. In general, our findings suggest that at a certain DEX concentration a peak of the synergistic mixture effect is reached, and the effect decreases with increasing DEX concentration via a type of down-regulating mechanism from thereon.

4.3 Time-Course study of a mixture

To evaluate the significance and effect of the time parameter, the EROD activity after combined treatment to BaP (0.1 µM) and DEX (2.5 µM) was tested for six different exposure times. To investigate the mixture effect and compare the results, a single substance exposure experiment (BaP 0.1 µM) was carried out, for each exposure time.

As Figure 8 indicates, we found there to be differences in EROD activity depending on the exposure duration. Under consideration of the low number of replicates and the standard deviation, as depicted in Figure 8, we can say that there appears to be a general increase in DEX-mediated potentiation of BaP-induced EROD activity, with increasing exposure time. Except for bars 3 and 4 (Figure 8, 6 h exposure), which shows a higher potentiation than seen for bars 7 & 8 (Figure 8, 18 h exposure), the data follows this trend.

Looking at previous studies on this matter, we find that a strict correlation between mixture effect and exposure time is not necessarily to be expected. As Celander et al. 1997 show, the correlation between mixture effect and exposure time does also depends on the composition of the mixture (Celander et al. 1997).

Overall, our findings suggest that the DEX-mediated potentiation of the BaP-induced CYP1A induction is active at an almost constant rate for at least 48 h of exposure. Therefore, the degree of potentiation increases over time.

4.4 Findings from comparing different glucocorticoids

To investigate whether different glucocorticoids behave differently, independently and in mixtures with AhR agonists, the EROD activity of cells treated with different combinations of BM, HYC, PRD with either BaP or BNF was tested.

As seen previously for DEX, cells treated with BM, HYC, and PRD, did not cause any significant EROD activity which suggests that none of the tested GR agonists is capable of inducing CYP1A in PLHC-I cells (Table 5, 14-34).

After combined treatment with BNF (0.1 µM), we observed that all glucocorticoids yield a similar, not statistically different (Table B1, 9-11), EROD activity (Figure 7). When administered combined with 0.1 µM of BaP, however, PRD causes a significantly lower activity than BM and HYC. A change in trend can be observed when looking at mixtures with higher AhR agonist concentration, where the involvement of BM causes the highest mixture effect both when added together with either BaP or BNF.

Previous studies have shown that combined treatment of mouse embryo cells with HYC + TCDD resulted in AhR-GR cross-reaction (Abbott 1995). It has also been shown that both DEX and BM enhance CYP1A mRNA and EROD activity in primary human placental trophoblast when combined with 3-MC (Stejskalová et al. 2013).

When comparing the results in Figure 7 to the results for DEX in Figure 6, it appears that there are clear differences in mixture effect depending on what glucocorticoid is involved. However, additional studies (Table 3), when BM, HYC, and PRD were each directly compared to DEX, show no statistically significant difference (Table 5, 40-45).

Overall, what our findings clearly indicate, is that an increase in EROD activity occurs in mixtures with all glucocorticoids tested. There appear to be differences in potency among the glucocorticoids which are, however, linked to the composition of the mixture and require further investigation.

4.5 Findings based on the treatment of pre-exposed cells.

To assess if the mixture effect changes after different exposure scenarios, BaP-pre-treated (24 h) cells exposed to DEX (24 h), were compared to those receiving the opposite treatment (Figure 9). Two mixtures with different BaP concentrations (0.1 and 1 µM) were tested each, while the DEX concentration stayed the same in all of them. To assess the mixture effect, a single substance exposure (48 h) of untreated cells was performed for both BaP concentrations.

Based on the results shown in Figure 9, we can say that after pre-treatment with BaP, a mixture effect can be observed for both BaP concentrations, while for the DEX pre-treatment experiment, all resulting EROD activities were statistically indifferent (Table D1, 5-8). While the mixture with the lower BaP

concentration caused a potentiation (~ 2-fold), the mixture with the higher BaP concentration caused a negative mixture effect, reaching only 30 % of the EROD activity seen for the control. Down-regulation of EROD activity at higher PAH levels in PLHC-I cells has been observed before (Celander et al. 1997).

Previous studies, investigating the interactions of TCDD and DEX, had shown evidence for a significant impact of DEX pre-treatment on the CYP1A induction via TCDD after 24 h of exposure of H4IIE rat hepatoma cells. According to Lai et al. (2003), a positively increasing mixture effect could be seen with increasing time of DEX pre-treatment (Lai et al. 2004). While considering that the experiments conducted by Lai et al. differ substantially from the experiments conducted in our studies (cell line, exposure time, AhR agonist, concentration), they show that DEX pre-exposure can be a factor to consider. Whether this applies to BaP and DEX in PHLC-I cells, must be assessed in future experiments.

Figure 10 shows another experiment, where pre-exposed cells (BNF 0.1 µM, 24 h) were treated with DEX. Besides testing different DEX concentrations, we also investigated the influence of the exposure duration with this experiment. As Figure 10 shows, statistically significant potentiation of EROD activity occurs after 24 h of treatment with DEX (1.25, 2.5, 5 µM) (Figure 10, 4-6). After 10 min. direct exposure of the cells to 1.25, 2.5 and 5 µM of DEX (Figure 10, 10-12), no significant difference to the vehicle control can be observed. Concentrations of 0.625 and 10 µM, appeared to even cause a slight inhibition of EROD activity after 10 min. exposure.

Inhibition was observed in every case when adding 1.25 and 2.5 µM of DEX, BM, HYC & PRD (24 h exposure) to BNF pre-exposed cells (0.1 µM, 24 h) in two separate experiments (Table 4). Previous studies also showed DEX-dependent inhibition after 10 min direct exposure of pre-treated (BNF 0.1 µM) PHLC-I cells (Wassmur et al. 2013).

4.6 Comparison of BaP and BNF as AhR agonists and their interaction with glucocorticoids.

As Figures 6 and 7 indicate, BNF appears to be a stronger CYP1A inducer after an exposure time of 24 h. As we can further derive from Figure 6, at low concentrations, both BaP and BNF react similarly with different DEX concentrations to yield comparable EROD activity. At higher AhR agonist concentration, the mixture effect is greater with BNF, rather than BaP, in the mixture. This observation can also be made when looking at Figure 7, indicating that the potency of AhR agonists, in combined treatment with glucocorticoids, is dependent on the concentration of the AhR agonist in the mixture. It has been shown, for different cell lines, that the difference in potency of BaP and BNF depends on factors like concentration (Bonacci 2003).

4.7 CYP1A mRNA production

After qPCR analysis of PLHC-I cells exposed to different chemicals and mixtures, we saw that the expression of CYP1A mRNA differs after exposure to BaP or BaP + DEX. As Figure 11 depicts, the mRNA production after BaP 0.1 µM treatment (24 h) is 2-fold compared to after exposure to BaP 0.1 µM + DEX 2.5 µM. An increase in DEX concentration appears to lead to an even lower expression of mRNA in the cells.

Figure 11 B indicates that a lower exposure time causes the relation between BaP and the mixture to flip, as the CYP1A mRNA level after mixture-treatment appears as ~1.2-fold of BaP.

Considering that the EROD data suggests that BaP + DEX do cause an increase in CYP1A, the results depicted in Figure 11 appear odd. However, the contrasting relation between BaP and the mixture may be due to metabolic reasons. If the mixture causes an increase in CYP1A induction early on (detected by EROD measurement and qPCR), the detoxification rate of BaP is therefore also increased. As the amount of BaP is decreasing in the cell, over time, the mRNA production slows down compared to cells treated only with BaP. While a high level of CYP1A may still be detectable (EROD assay), the level of mRNA produced is dropping earlier on and is therefore suddenly lower after mixture treatment, than after treatment with BaP.

There is little research done on how the combined treatment with BaP + DEX affect the CYP1A expression in fish species; however, as Sonneveld et al. (2007) describes, DEX causes an increase in BaP-induced CYP1A expression in hepatic rat cells (H4IIe) after 24 h of combined exposure, while the level of expression does not change in human cells (HepG2 and T47D) (Sonneveld et al. 2007).

By interpreting the results displayed in Figure 11, the low number of replicates must be considered. Hence, these results can only be regarded as preliminary indications.

4.8 Intracellular BaP levels

Figure 12 shows the difference in intracellular BaP levels after analysis of cells exposed for different duration to different treatments. While the BaP levels are similar or even lower compared to the control, after mixture treatment involving a lower BaP concentration (0.1 µM), DEX causes higher BaP levels when added in combination with 1 µM of BaP. This suggests that depending on the BaP concentration, DEX can slow down the metabolism or elimination rate of BaP, causing higher BaP levels to remain in the cell.

5. Conclusion

To assess the mixture effect of BaP and DEX, several experiments were conducted, measuring the CYP1A activity (EROD assay) and the CYP1A mRNA abundance (qPCR) in PHLC-I cells. Treatments of cells were performed using different combinations of substances, in different compositions, for varying exposure durations. Also, the difference in exposure of pre-accommodated and untreated cells was investigated. To put our findings on the behaviour of BaP and DEX in perspective, we further conducted experiments utilizing additional compounds of their respective chemical classes (BNF and BM, HYC, PRD, respectively).

We have seen, that in contrast to the AhR agonists BaP and BNF, the glucocorticoids and GR agonists DEX, BM, HYC and PRD, do not induce significant CYP1A activity when applied alone. Previous studies on DEX in PHLC-I cells reached the conclusion that DEX has a negligible capacity of inducing CYP1A (Celander et al. 1997).

Furthermore, we conclude that DEX, BM, HYC and PRD, when applied together with BaP or BNF, do cause a potentiation of CYP1A induction in untreated PHLC-I cells, compared to after a single substance exposure to the same concentration, of the respective AhR agonist, as present in the mixture. The degree of potentiation appeared elevated when, (A) the concentration AhR agonist was higher; (B) BNF was the AhR-agonist present in the mixture; (C) the glucocorticoid concentration in the mixture was lower (regarding mixtures with DEX); (D) when BM was the glucocorticoid present in the mixture. It has been shown before, that DEX enhances the BNF-induced CYP1A activity in PHLC-I cells (Celander et al. 1997). A mixture effect on the CYP1A activity after the combined treatment with DEX and BaP has also been reported; however, in mammalian cells (Dvořák et al. 2008).

Regarding the time parameter, we have found preliminary indication of an increasing, potentiating mixture effect of BaP + DEX, with increasing exposure duration. This conclusion stands in contrast to what has been described earlier for the behaviour of a mixture of BNF and DEX in the same system. However, literature further indicates that the correlation between mixture effect and time exposure also varies depending on the mixture composition (Celander et al. 1997). Due to the small number of replicates, we were able to produce, we cannot present any significant data.

After comparing the mixture effect on CYP1A activity following different scenarios of exposing pre-treated cells, we conclude that the pre-exposure to DEX does not cause a significant enhancement of CYP1A induction. DEX-treatment of cells that have been accommodated to BaP, however, does cause a mixture effect, which appeared positive after adding a lower BaP concentration and negative when pre-treating the cells with a higher BaP concentration. A negative mixture effect can also be seen after treatment of BNF-pre-exposed cells with different concentrations of BM, HYC and PRD

respectively. The same has been done for DEX, where we learned that not only a difference in concentration but also in exposure duration leads to a difference in mixture effect.

We were able to show that the CYP1A mRNA production is altered when treating cells with BaP + DEX instead of BaP only. After 3 h exposure, the mixture treatment resulted in a higher amount of mRNA, whereas after 24 h exposure, the mRNA level was lower compared to the control, as our pilot experiments indicate. For this cell line, no information on the impact of BaP + DEX on CYP1A mRNA has been published yet. Our findings stand in contrast to what has been described previously for hepatic rat cells after 24 h exposure (Sonneveld et al. 2007).

Given our results and the findings, the qPCR results in particular, we can hypothesize that the presence of DEX causes increased elimination of BaP from the cell. Our analysis of the intracellular BaP levels (Figure 12) do not strictly exclude this hypothesis, but it must be considered that the effect DEX has on the elimination rate of BaP, may vary depending on the mixture composition; especially the BaP concentration, as seen in Figure 12.

As a final remark we can say that the findings presented in this thesis are, to a great extent, to be considered as preliminary indications on the behaviour of BaP + DEX in fish species. Further studies should aim to reproduce and verify the results presented and to elucidate additional aspects on how the interaction of BaP and DEX unfolds. Promising endpoints to investigate could be the mixture effect on the cell efflux and GR-mediated expression. With respect to environmental relevance, the testing of lower DEX concentrations should also be considered, as the concentrations utilized in the experiments presented here, exceed concentrations commonly detected in environmental matrices.

5.1 Conflict of Interest

None

6. References

Abbott, B. D. (1995): Review of the interaction between TCDD and glucocorticoids in embryonic palate. In *Toxicology* 105 (2-3), pp. 365–373. DOI: 10.1016/0300-483X(95)03234-7.

Abel, Josef; Haarmann-Stemmann, Thomas (2010): An introduction to the molecular basics of aryl hydrocarbon receptor biology. In *Biological chemistry* 391 (11), pp. 1235–1248. DOI: 10.1515/bc.2010.128.

ATCC (2022): PLHC-1. CRL-2406™. ATCC. Available online at https://www.atcc.org/products/crl-2406, updated on 2022, checked on 4/20/2022.

Backhaus, Thomas; Karlsson, Maja (2014): Screening level mixture risk assessment of pharmaceuticals in STP effluents. In *Water research* 49, pp. 157–165. DOI: 10.1016/j.watres.2013.11.005.

Bielefeld, Kirsten A.; Lee, Chunja; Riddick, David S. (2008): Regulation of aryl hydrocarbon receptor expression and function by glucocorticoids in mouse hepatoma cells. In *Drug metabolism and disposition: the biological fate of chemicals* 36 (3), pp. 543–551. DOI: 10.1124/dmd.107.019703.

Bio-Rad Laboratories, Inc. (2022): What is Real-Time PCR (qPCR)? Edited by Inc. Bio-Rad Laboratories. Available online at https://www.bio-rad.com/en-se/applications-technologies/what-real-time-pcr-qpcr?ID=LUSO4W8UU, updated on 2022, checked on 3/1/2022.

Bonacci, S. (2003): Induction of EROD activity in European eel (Anguilla anguilla) experimentally exposed to benzo[a]pyrene and β-naphthoflavone. In *Environment International* 29 (4), pp. 467–473. DOI: 10.1016/S0160-4120(03)00005-9.

Burkina, Viktoriia; Sakalli, Sidika; Rasmussen, Martin Krøyer; Zamaratskaia, Galia; Koba, Olga; Thai, Giang Pham et al. (2015): Does dexamethasone affect hepatic CYP450 system of fish? Semi-static in-vivo experiment on juvenile rainbow trout. In *Chemosphere* 139, pp. 155–162. DOI: 10.1016/j.chemosphere.2015.06.031.

Celander, M.; Hahn, M. E.; Stegeman, J. J. (1996): Cytochromes P450 (CYP) in the Poeciliopsis lucida hepatocellular carcinoma cell line (PLHC-1): dose- and time-dependent glucocorticoid potentiation of CYP1A induction without induction of CYP3A. In *Archives of biochemistry and biophysics* 329 (1), pp. 113–122. DOI: 10.1006/abbi.1996.0198.

Celander, Malin; Bremer, Jessica; Hahn, Mark E.; Stegeman, John J. (1997): Glucocorticoid-xenobiotic interactions: Dexamethasone-mediated potentiation of cytochrome P4501A induction by β-naphthoflavone in a fish hepatoma cell line (PLHC-1). In *Environ Toxicol Chem* 16 (5), pp. 900–907. DOI: 10.1002/etc.5620160509.

Collins, J. F.; Brown, J. P.; Dawson, S. V.; Marty, M. A. (1991): Risk assessment for benzo[a]pyrene. In *Regulatory Toxicology and Pharmacology* 13 (2), pp. 170–184. DOI: 10.1016/0273-2300(91)90020-V.

DellaGreca, Marina; Fiorentino, Antonio; Isidori, Marina; Lavorgna, Margherita; Previtera, Lucio; Rubino, Maria; Temussi, Fabio (2004): Toxicity of prednisolone, dexamethasone and their photochemical derivatives on aquatic organisms. In *Chemosphere* 54 (5), pp. 629–637. DOI: 10.1016/j.chemosphere.2003.09.008.

Dvořák, Z.; Vrzal, R.; Pávek, P.; Ulrichová, J. (2008): An evidence for regulatory cross-talk between aryl hydrocarbon receptor and glucocorticoid receptor in HepG2 cells. In *Physiological research* 57 (3), pp. 427–435. DOI: 10.33549/physiolres.931090.

Entringer S. (1996): Dexamethasone. Edited by Inc. Cerner Multum. Available online at https://www.drugs.com/dexamethasone.html, updated on 10/19/2021, checked on 11/29/2021.

Fallahi, Shirin; Mlnaříková, Marie; Alvord, Charlotte; Alendal, Guttorm; Frøysa, Håvard G.; Lundh, Torbjörn; Celander, Malin C. (2020): New Conceptual Toxicokinetic Model to Assess Synergistic

Mixture Effects between the Aromatic Hydrocarbon β-Naphthoflavone and the Azole Nocodazole on the CYP1A Biomarker in a Fish Cell Line. In *Environmental science & technology* 54 (21), pp. 13748–13758. DOI: 10.1021/acs.est.0c04839.

Farrell, Chloe; O'Keane, Veronica (2016): Epigenetics and the glucocorticoid receptor: A review of the implications in depression. In *Psychiatry research* 242, pp. 349–356. DOI: 10.1016/j.psychres.2016.06.022.

Guengerich, F. Peter (2008): Cytochrome p450 and chemical toxicology. In *Chemical research in toxicology* 21 (1), pp. 70–83. DOI: 10.1021/tx700079z.

Hankinson, O. (1995): The aryl hydrocarbon receptor complex. In *Annual review of pharmacology and toxicology* 35, pp. 307–340. DOI: 10.1146/annurev.pa.35.040195.001515.

Hattemer-Frey, H. A.; Travis, C. C. (1991): Benzo-a-pyrene: environmental partitioning and human exposure. In *Toxicology and industrial health* 7 (3), pp. 141–157. DOI: 10.1177/074823379100700303.

Honour, John W. (2006): Gas chromatography-mass spectrometry. In *Methods in molecular biology (Clifton, N.J.)* 324, pp. 53–74. DOI: 10.1385/1-59259-986-9:53.

Ibarra, David; Martín-Sampedro, Raquel; Wicklein, Bernd; Borrero-López, Antonio M.; Valencia, Concepción; Valdehíta, Ana et al. (2021): Populus alba L., an Autochthonous Species of Spain: A Source for Cellulose Nanofibers by Chemical Pretreatment. In *Polymers* 14 (1). DOI: 10.3390/polym14010068.

Jana, Snehasis; Paliwal, Jyoti (2007): Molecular mechanisms of cytochrome p450 induction: potential for drug-drug interactions. In *Current protein & peptide science* 8 (6), pp. 619–628. DOI: 10.2174/138920307783018668.

Kapitulnik, J.; Levin, W.; Conney, A. H.; Yagi, H.; Jerina, D. M. (1977): Benzoapyrene 7,8-dihydrodiol is more carcinogenic than benzoapyrene in newborn mice. In *Nature* 266 (5600), pp. 378–380. DOI: 10.1038/266378a0.

Krieger, Stephen; Sorrells, Shawn F.; Nickerson, Molly; Pace, Thaddeus W. W. (2014): Mechanistic insights into corticosteroids in multiple sclerosis: war horse or chameleon? In *Clinical neurology and neurosurgery* 119, pp. 6–16. DOI: 10.1016/j.clineuro.2013.12.021.

Lai, K. P.; Wong, M. H.; Wong, Chris K. C. (2004): Modulation of AhR-mediated CYP1A1 mRNA and EROD activities by 17beta-estradiol and dexamethasone in TCDD-induced H411E cells. In *Toxicological sciences : an official journal of the Society of Toxicology* 78 (1), pp. 41–49. DOI: 10.1093/toxsci/kfh045.

Lammers, Twan; Sofias, Alexandros Marios; van der Meel, Roy; Schiffelers, Raymond; Storm, Gert; Tacke, Frank et al. (2020): Dexamethasone nanomedicines for COVID-19. In *Nature nanotechnology* 15 (8), pp. 622–624. DOI: 10.1038/s41565-020-0752-z.

Larigot, Lucie; Juricek, Ludmila; Dairou, Julien; Coumoul, Xavier (2018): AhR signaling pathways and regulatory functions. In *Biochimie open* 7, pp. 1–9. DOI: 10.1016/j.biopen.2018.05.001.

Lindim, C.; Zwart, D. de; Cousins, I. T.; Kutsarova, S.; Kühne, R.; Schüürmann, G. (2019): Exposure and ecotoxicological risk assessment of mixtures of top prescribed pharmaceuticals in Swedish freshwaters. In *Chemosphere* 220, pp. 344–352. DOI: 10.1016/j.chemosphere.2018.12.118.

Manikandan, Palrasu; Nagini, Siddavaram (2018): Cytochrome P450 Structure, Function and Clinical Significance: A Review. In *Current drug targets* 19 (1), pp. 38–54. DOI: 10.2174/1389450118666170125144557.

McCracken, G. H.; Lebel, M. H. (1989): Dexamethasone therapy for bacterial meningitis in infants and children. In *American journal of diseases of children (1960)* 143 (3), pp. 287–289. DOI: 10.1001/archpedi.1989.02150150041013.

Monostory, Katalin; Kohalmy, Krisztina; Prough, Russell A.; Kóbori, László; Vereczkey, László (2005): The effect of synthetic glucocorticoid, dexamethasone on CYP1A1 inducibility in adult rat and human hepatocytes. In *FEBS letters* 579 (1), pp. 229–235. DOI: 10.1016/j.febslet.2004.11.080.

Musee, Ndeke; Kebaabetswe, Lemme Prica; Tichapondwa, Shepherd; Tubatsi, Gosaitse; Mahaye, Ntombikayise; Leareng, Samuel Keeng; Nomngongo, Philiswa Nosizo (2021): Occurrence, Fate, Effects, and Risks of Dexamethasone: Ecological Implications Post-COVID-19. In *International journal of environmental research and public health* 18 (21). DOI: 10.3390/ijerph182111291.

Pascussi, J. M.; Drocourt, L.; Fabre, J. M.; Maurel, P.; Vilarem, M. J. (2000): Dexamethasone induces pregnane X receptor and retinoid X receptor-alpha expression in human hepatocytes: synergistic increase of CYP3A4 induction by pregnane X receptor activators. In *Molecular pharmacology* 58 (2), pp. 361–372. DOI: 10.1124/mol.58.2.361.

Petrulis, J. R.; Chen, G.; Benn, S.; LaMarre, J.; Bunce, N. J. (2001): Application of the ethoxyresorufin-O-deethylase (EROD) assay to mixtures of halogenated aromatic compounds. In *Environmental toxicology* 16 (2), pp. 177–184. DOI: 10.1002/tox.1022.

Smoak, Kathleen A.; Cidlowski, John A. (2004): Mechanisms of glucocorticoid receptor signaling during inflammation. In *Mechanisms of ageing and development* 125 (10-11), pp. 697–706. DOI: 10.1016/j.mad.2004.06.010.

Sonneveld, Edwin; Jonas, Arjen; Meijer, Onno C.; Brouwer, Abraham; van der Burg, Bart (2007): Glucocorticoid-enhanced expression of dioxin target genes through regulation of the rat aryl hydrocarbon receptor. In *Toxicological sciences : an official journal of the Society of Toxicology* 99 (2), pp. 455–469. DOI: 10.1093/toxsci/kfm176.

Stejskalová, Lucie; Vrzal, Radim; Rulcová, Alice; Dvořák, Zdeněk; Pávek, Petr (2013): Effects of glucocorticoids on cytochrome P450 1A1 (CYP1A1) expression in isolated human placental trophoblast. In *J Appl Biomed* 11 (3), pp. 163–172. DOI: 10.2478/v10136-012-0022-y.

Sun, Lingli; Xu, Wei; He, Jiangyan; Yin, Zhan (2010): In vivo alternative assessment of the chemicals that interfere with anterior pituitary POMC expression and interrenal steroidogenesis in POMC: EGFP transgenic zebrafish. In *Toxicology and applied pharmacology* 248 (3), pp. 217–225. DOI: 10.1016/j.taap.2010.08.015.

Ukić, Š.; Sigurnjak, M.; Cvetnić, M.; Markić, M.; Stankov, M. Novak; Rogošić, M. et al. (2019): Toxicity of pharmaceuticals in binary mixtures: Assessment by additive and non-additive toxicity models. In *Ecotoxicology and environmental safety* 185, p. 109696. DOI: 10.1016/j.ecoenv.2019.109696.

Wang, Shao-Hung; Liang, Chu-Ting; Liu, Yi-Wen; Huang, Min-Cong; Huang, See-Chang; Hong, Wei-Fu; Su, Jyan-Gwo J. (2009): Crosstalk between activated forms of the aryl hydrocarbon receptor and glucocorticoid receptor. In *Toxicology* 262 (2), pp. 87–97. DOI: 10.1016/j.tox.2009.03.020.

Wassmur, Britt; Gräns, Johanna; Norström, Elisabeth; Wallin, Margareta; Celander, Malin C. (2013): Interactions of pharmaceuticals and other xenobiotics on key detoxification mechanisms and cytoskeleton in Poeciliopsis lucida hepatocellular carcinoma, PLHC-1 cell line. In *Toxicology in vitro : an international journal published in association with BIBRA* 27 (1), pp. 111–120. DOI: 10.1016/j.tiv.2012.10.002.

Yennurajalingam, Sriram; Frisbee-Hume, Susan; Palmer, J. Lynn; Delgado-Guay, Marvin O.; Bull, Janet; Phan, Alexandria T. et al. (2013): Reduction of cancer-related fatigue with dexamethasone: a double-blind, randomized, placebo-controlled trial in patients with advanced cancer. In *Journal of clinical oncology : official journal of the American Society of Clinical Oncology* 31 (25), pp. 3076–3082. DOI: 10.1200/JCO.2012.44.4661.

Supplement:

List of chemicals

Table 2: List of chemicals used in the experiments described and relevant information about them.

Chemical	Formula	CAS number	Characteristics	Company	Purity
Acetone	$(CH_3)_2CO$	67-64-1	Irritant, flammable, damaging to the respiratory system	Merck	p.a.
Acetonitrile	CH_3CN	75- 05- 8	Acute and chronic health hazard, highly flammable, toxic to aquatic environment	Merck	p.a.
Benzo[a]pyrene		50-32-8	CMR toxic	Sigma	≥ 96%
Beta- Naphthoflavone		6051-87- 2	Irritant	Sigma	97%
Beta- mercaptoethanol		60-24-2	Irritant, combustible, flammable Reproductive toxic, harmful if swallowed/inhaled,	Sigma	> 99%
Betamethasone		378-44-9	CMR toxic	Sigma	≥ 98%
Bovine Serum Albumin (BSA)	-	9048-46- 8	Harmful if swallowed	Sigma	≥ 98%
Dexamethasone		50-02-2	CMR toxic	Sigma	≥ 97 %
Dimethyl sulfoxide (DMSO)	C_2H_6OS	67-68-5	-	Sigma	≥ 99.9%
Disodium hydrogen phosphate	Na_2HPO_4	7558-79- 4	-	Sigma	p.a.
EDTA	$C_{10}H_{16}N_2O_8$	60-00-4	Acute and chronic health hazard, Combustible, toxic to aquatic environment	Sigma	99-101%
Ethanol (EtOH)	CH_3CH_2OH	64-17-5	Acute and chronic health hazard, highly flammable	Sigma	n.a.
7-Ethoxyresorufin (ER)	$C_{14}H_{11}NO_3$	5725-91- 7	-	Sigma	p.a.
Fetal Bovine Serum (FBS)	-	-	-	Thermo Fisher	Premium Plus
Fluorescamine	$C_{17}H_{10}O_4$	38183-12-9	-	Sigma	≥ 98%

Heptane	C_7H_{16}	142-82-5	Irritant, damaging to the respiratory system	Sigma	99%
2- [4-(2-Hydroxyethyl)-1-piperazine] ethane sulfonic acid (HEPES)	-	7365-45- 9	Avoid breathing dust/fume/gas/mist/vapours/spray, Use only outdoors or in a well- ventilated area	Sigma	≥ 99.5%
Hydrochloric Acid	HCl	7647- 01-0	Corrosive, harmful	Sigma	n.a.
Hydrocortisone		50-23-7	CMR toxic	Sigma	≥ 98%
Minimum Essential Media (MEM) Powder	-	-	-	Sigma	n.a.
Methanol (MeOH)	CH_3OH	67-56-1	Acute and chronic health hazard, highly flammable	Sigma	≥ 99.9%
Sodium Hydroxide	NaOH	1310-73- 2	corrosive	Sigma	p.a.
Potassium chloride	KCl	7447-40- 7	-	Merck	p.a.
Potassium dihydrogen phosphate	KH_2PO_4	7778-77- 0	-	Merck	p.a.
Prednisolone		50-24-8	CMR toxic	Sigma	≥ 99%
7- Hydroxy-3H-phenoxazin-3-one-10-oxide sodium salt (Resazurin sodium salt)	$C_{12}H_6NNaO_4$	62758-13-8	Harmful	n.a.	n.a.
Resorufin	$C_{12}H_7NO_3$	635-78-9	Acute and chronic health hazard	n.a.	n.a.
Sodium chloride	NaCl	7440-23-5	-	Merck	p.a.
Sodium bicarbonate	$NaHCO_3$	144-55-8	-	Sigma	p.a.
Sodium hydrogen phosphate dodecahydrate	$Na_2HPO_4x12\ H_2O$	10039 -32-4	-	Merck	p.a.
Trypsin		07-07-9002	Harmful, CMR toxic	Thermo Fisher	n.a.

Additional Experimental Data

Table 3: Data of the Results of EROD experiments carried out on the 13.12.2022.

Treatment	Concentration [µM]	Number of Replicates	Mean specific EROD activity [pmol protein min^{-1}]	Standard Deviation	Normalized Mean Specific EROD activity	Standard Deviation
BaP	0.10	8	52.577	7.909	1.00	0.14
BNF	0.10	8	34.719	9.882	0.66	0.18
DEX	2.50	4	18.076	4.558	0.34	0.08
BM	2.50	4	- 0.301	1.044	- 0.01	0.02
BaP + DEX	0.1 + 2.5	4	88.534	4.993	1.68	0.08
BaP + BM	0.1 + 2.5	4	100.892	19.724	1.92	0.32
BNF + DEX	0.1 + 2.5	4	99.237	17.936	1.89	0.30
BNF + BM	0.1 + 2.5	4	107.901	8.948	2.05	0.15
BaP	0.10	8	67.936	15.053	1.00	0.21
BNF	0.10	8	112.935	45.010	1.66	0.62
DEX	2.50	4	47.375	13.795	0.70	0.18
HYC	2.50	4	- 0.062	0.388	0.00	0.00
BaP + DEX	0.1 + 2.5	4	129.570	12.149	1.91	0.15
BaP + HYC	0.1 + 2.5	4	94.480	17.805	1.39	0.23
BNF + DEX	0.1 + 2.5	4	119.939	18.529	1.77	0.24
BNF + HYC	0.1 + 2.5	4	118.172	27.969	1.74	0.36
BaP	0.10	8	43.837	9.281	1.00	0.20
BNF	0.10	8	7.315	1.145	0.17	0.02
DEX	2.50	4	10.880	20.007	0.25	0.40
PRD	2.50	4	0.640	0.479	0.01	0.01
BaP + DEX	0.1 + 2.5	4	47.263	3.569	1.08	0.07
BaP + PRD	0.1 + 2.5	4	48.755	8.085	1.11	0.16
BNF + DEX	0.1 + 2.5	4	65.454	15.220	1.49	0.30
BNF + PRD	0.1 + 2.5	4	58.268	22.282	1.33	0.44

Table 4: Data of the EROD experiments carried out on the 08.12.2021. The treatments were performed after BNF pre-exposure (0.1 µM, 24 h). The exposure time of the treatments was 10 min.

Treatment	Concentration [µM]	Number of Replicates	Mean specific EROD activity [pmol protein min^{-1}]	Standard Deviation	Normalized Mean Specific EROD activity	Standard Deviation
DMSO	0.10	8	155.165	21.858	1.00	0.13
DEX	2.50	4	88.048	30.519	0.57	0.17
BM	2.50	4	87.527	17.877	0.56	0.10
HYC	2.50	4	69.428	13.560	0.45	0.08
PRD	2.50	4	126.505	27.384	0.82	0.15
DMSO	0.10	8	164.101	30.162	1.00	0.17
DEX	1.25	4	99.154	13.904	0.60	0.07
BM	1.25	4	83.488	12.335	0.51	0.07
HYC	1.25	4	97.329	6.369	0.59	0.03
PRD	1.25	4	98.753	15.124	0.60	0.08

Supplementary Statistical Data

Table 5: Statistical analysis table comparing two datasets each using the Wilcoxon test (95% confidence interval).

#	Displayed	Date	Plate number	Exposure Time [h]	Treatment 1 (Replicates)	Treatment 2 (Replicates)	p-value (Wilcoxon test)
1	-	02.03.22	1	24	DMSO (4)	DEX 2.5 µM (3)	1.00
2	-	28.01.22	1	24	DMSO (4)	DEX 2.5 µM (4)	0.49
3	-	28.01.22	1	24	DMSO (4)	DEX 5 µM (4)	0.34
4	-	28.01.22	1	24	DMSO (4)	DEX 10 µM (4)	0.89
5	-	28.01.22	2	24	DMSO (4)	DEX 2.5 µM (4)	1.00
6	-	28.01.22	2	24	DMSO (4)	DEX 5 µM (4)	0.69
7	-	28.01.22	2	24	DMSO (4)	DEX 10 µM (4)	0.69
8	-	28.01.22	3	24	DMSO (4)	DEX 2.5 µM (4)	0.49
9	-	28.01.22	3	24	DMSO (4)	DEX 5 µM (4)	0.89
10	-	28.01.22	3	24	DMSO (4)	DEX 10 µM (4)	1.00
11	-	28.01.22	4	24	DMSO (4)	DEX 2.5 µM (4)	0.34
12	-	28.01.22	4	24	DMSO (4)	DEX 5 µM (4)	0.49
13	-	28.01.22	4	24	DMSO (4)	DEX 10 µM (4)	0.34
14	-	24.02.22	1	24	DMSO (4)	BM 2.5 µM (4)	0.49
15	-	24.02.22	1	24	DMSO (4)	HYC 2.5 µM (4)	0.89
16	-	24.02.22	1	24	DMSO (4)	PRD 2.5 µM (4)	0.89
17	-	24.02.22	2	24	DMSO (4)	BM 2.5 µM (4)	0.34
18	-	24.02.22	2	24	DMSO (4)	HYC 2.5 µM (4)	0.20
19	-	24.02.22	2	24	DMSO (4)	PRD 2.5 µM (4)	0.34
20	-	24.02.22	3	24	DMSO (4)	BM 2.5 µM (4)	1.00
21	-	24.02.22	3	24	DMSO (4)	HYC 2.5 µM (4)	0.03
22	-	24.02.22	3	24	DMSO (4)	PRD 2.5 µM (4)	1.00
23	-	24.02.22	4	24	DMSO (4)	BM 2.5 µM (4)	0.11
24	-	24.02.22	4	24	DMSO (4)	HYC 2.5 µM (4)	0.11
25	-	24.02.22	4	24	DMSO (4)	PRD 2.5 µM (4)	0.49
26	-	21.03.22	1	24	DMSO (4)	BM 2.5 µM (4)	0.03*

27	-	21.03.22	1	24	DMSO (4)	HYC 2.5 μM (4)	0.03*
28	-	21.03.22	1	24	DMSO (4)	PRD 2.5 μM (4)	0.03*
29	-	21.03.22	2	24	DMSO (4)	BM 2.5 μM (4)	0.03*
30	-	21.03.22	2	24	DMSO (4)	HYC 2.5 μM (4)	0.03*
31	-	21.03.22	2	24	DMSO (4)	PRD 2.5 μM (4)	0.03*
32	-	21.03.22	3	24	DMSO (4)	BM 2.5 μM (4)	0.03*
33	-	21.03.22	3	24	DMSO (4)	HYC 2.5 μM (4)	0.03*
34	-	21.03.22	3	24	DMSO (4)	PRD 2.5 μM (4)	0.03*
35	-	02.03.22	1	48	DMSO (4)	DEX 2.5 μM (4)	0.69
36	-	02.03.22	1	18	DMSO (4)	DEX 2.5 μM (4)	1.00
37	-	02.03.22	2	6	DMSO (4)	DEX 2.5 μM (4)	0.34
38	-	02.03.22	2	3	DMSO (4)	DEX 2.5 μM (4)	0.06
39	-	02.03.22	2	0.16	DMSO (4)	DEX 2.5 μM (4)	0.69
40	Table 3	13.12.21	1	24	BaP 0.1 μM + DEX 2.5 μM (4)	BaP 0.1 μM + BM 2.5 μM (4)	0.34
41	Table 3	13.12.21	1	24	BNF 0.1 μM + DEX 2.5 μM (4)	BNF 0.1 μM + BM 2.5 μM (4)	0.34
42	Table 3	13.12.21	2	24	BaP 0.1 μM + DEX 2.5 μM (4)	BaP 0.1 μM + HYC 2.5 μM (4)	0.05
43	Table 3	13.12.21	2	24	BNF 0.1 μM + DEX 2.5 μM (4)	BNF 0.1 μM + HYC 2.5 μM (4)	0.89
44	Table 3	13.12.21	3	24	BaP 0.1 μM + DEX 2.5 μM (4)	BaP 0.1 μM + PRD 2.5 μM (4)	0.69
45	Table 3	13.12.21	3	24	BNF 0.1 μM + DEX 2.5 μM (4)	BNF 0.1 μM + PRD 2.5 μM (4)	0.69
46	Table 4	08.12.21	1	24.16 + 0.16	BNF 0.1 μM + DEX 2.5 μM (4)	BNF 0.1 μM + BM 2.5 μM (4)	0.69
47	Table 4	08.12.21	1	24.16 + 0.16	BNF 0.1 μM + DEX 2.5 μM (4)	BNF 0.1 μM + HYC 2.5 μM (4)	0.34
48	Table 4	08.12.21	1	24.16 + 0.16	BNF 0.1 μM + DEX 2.5 μM (4)	BNF 0.1 μM + PRD 2.5 μM (4)	0.20
49	Table 4	08.12.21	1	24.16 + 0.16	BNF 0.1 μM + BM 2.5 μM (4)	BNF 0.1 μM + HYC 2.5 μM (4)	0.20
50	Table 4	08.12.21	1	24.16 + 0.16	BNF 0.1 μM + BM 2.5 μM (4)	BNF 0.1 μM + PRD 2.5 μM (4)	0.06
51	Table 4	08.12.21	1	24.16 + 0.16	BNF 0.1 μM + HYC 2.5 μM (4)	BNF 0.1 μM + PRD 2.5 μM (4)	0.03
52	Table 4	08.12.21	2	24.16 + 0.16	BNF 0.1 μM + DEX 1.25 μM (4)	BNF 0.1 μM + BM 1.25 μM (4)	0.20
53	Table 4	08.12.21	2	24.16 + 0.16	BNF 0.1 μM + DEX 1.25 μM (4)	BNF 0.1 μM + HYC 1.25 μM (4)	1.00
54	Table 4	08.12.21	2	24.16 + 0.16	BNF 0.1 μM + DEX 1.25 μM (4)	BNF 0.1 μM + PRD 1.25 μM (4)	0.89
55	Table 4	08.12.21	2	24.16 + 0.16	BNF 0.1 μM + BM 1.25 μM (4)	BNF 0.1 μM + HYC 1.25 μM (4)	0.20
56	Table 4	08.12.21	2	24.16 + 0.16	BNF 0.1 μM + BM 1.25 μM (4)	BNF 0.1 μM + PRD 1.25 μM (4)	0.34
57	Table 4	08.12.21	2	24.16 + 0.16	BNF 0.1 μM + HYC 1.25 μM (4)	BNF 0.1 μM + PRD 1.25 μM (4)	1.00

* The mean average EROD activity higher after DMSO treatment.

Figure 6:

Table A: Normalized mean EROD activity as depicted in Figure 6.

Treatment	Norm. mean specific EROD activity	Standard deviation (+-)
BaP 0.1 µM	1.00	0.23
BaP 0.1 µM + DEX 2.5 µM	1.57	0.37
BaP 0.1 µM + DEX 5 µM	1.81	0.57
BaP 0.1 µM + DEX 10 µM	1.57	0.59
BaP 0.5 µM	2.29	0.76
BaP 0.5 µM + DEX 2.5 µM	3.49	0.79
BaP 0.5 µM + DEX 5 µM	2.57	0.80
BaP 0.5 µM + DEX 10 µM	2.62	0.89
BNF 0.1 µM	1.00	0.28
BNF 0.1 µM + DEX 2.5 µM	1.76	0.47
BNF 0.1 µM + DEX 5 µM	1.63	0.49
BNF 0.1 µM + DEX 10 µM	1.93	0.24
BNF 0.5 µM	6.05	1.80
BNF 0.5 µM + DEX 2.5 µM	13.5	4.07
BNF 0.5 µM + DEX 5 µM	10.64	2.17
BNF 0.5 µM + DEX 10 µM	7.12	1.77

Table A1: Statistical analysis of datasets from the experiment(s) depicted in Figure 6, applying the Wilcoxon test (95% confidence interval).

#	Treatment 1 (Replicates)	Treatment 2 (Replicates)	p- value (Wilcoxon-test)
1	BaP 0.1 µM +DEX 2.5 µM (16)	BaP 0.1 µM + DEX 5 µM (16)	0.36
2	BaP 0.1 µM +DEX 2.5 µM (16)	BaP 0.1 µM + DEX 10 µM (16)	0.54
3	BaP 0.1 µM + DEX 5 µM (16)	BaP 0.1 µM + DEX 10 µM (16)	0.34
4	BNF 0.5 µM + DEX 2.5 µM (8)	BNF 0.5 µM + DEX 5 µM (8)	0.16
5	BNF 0.5 µM + DEX 2.5 µM (8)	BNF 0.5 µM + DEX 10 µM (8)	0.001
6	BNF 0.5 µM + DEX 5 µM (8)	BNF 0.5 µM + DEX 10 µM (8)	0.005
7	BaP 0.5 µM +DEX 2.5 µM (16)	BaP 0.5 µM + DEX 5 µM (16)	0.01
8	BaP 0.5 µM +DEX 2.5 µM (16)	BaP 0.5 µM + DEX 10 µM (16)	0.01
9	BaP 0.5 µM + DEX 5 µM (16)	BaP 0.5 µM + DEX 10 µM (16)	0.93
10	BNF 0.1 µM +DEX 2.5 µM (16)	BNF 0.5 µM + DEX 10 µM (16)	0.33
11	BNF 0.1 µM + DEX 5 µM (16)	BNF 0.1 µM + DEX 10 µM (16)	0.08
12	BaP 0.1 µM +DEX 2.5 µM (16)	BaP 0.1 µM + DEX 5 µM (16)	0.36
13	BaP 0.1 µM +DEX 2.5 µM (16)	BaP 0.1 µM + DEX 10 µM (16)	0.54
14	BaP 0.1 µM + DEX 5 µM (16)	BaP 0.1 µM + DEX 10 µM (16)	0.34
15	BNF 0.5 µM + DEX 2.5 µM (8)	BNF 0.5 µM + DEX 5 µM (8)	0.16
16	BaP 0.1 µM (12)	BaP 0.1 µM + DEX 2.5 µM (16)	$3.71 * 10^{-4}$
17	BaP 0.1 µM (12)	BaP 0.1 µM + DEX 5 µM (16)	$2.01 * 10^{-4}$
18	BaP 0.1 µM (12)	BaP 0.1 µM + DEX 10 µM (16)	$3.64 * 10^{-3}$
19	BaP 0.5 µM (16)	BaP 0.5 µM + DEX 2.5 µM (16)	$4.67 * 10^{-4}$
20	BaP 0.5 µM (16)	BaP 0.5 µM + DEX 5 µM (16)	0.42
21	BaP 0.5 µM (16)	BNF 0.5 µM + DEX 10 µM (8)	0.32
22	BNF 0.1 µM (8)	BNF 0.1 µM + DEX 2.5 µM (8)	$4.66 * 10^{-3}$
23	BNF 0.1 µM (8)	BNF 0.1 µM + DEX 5 µM (8)	$6.90 * 10^{-3}$
24	BNF 0.1 µM (8)	BNF 0.1 µM + DEX 10 µM (8)	$3.11 * 10^{-4}$
25	BNF 0.5 µM (8)	BNF 0.5 µM + DEX 2.5 µM (8)	$6.22 * 10^{-4}$
26	BNF 0.5 µM (8)	BNF 0.5 µM + DEX 5 µM (8)	$1.10 * 10^{-3}$
27	BNF 0.5 µM (8)	BNF 0.5 µM + DEX 10 µM (8)	0.28

Figure 7

Table B: Normalized mean EROD activity as depicted in Figure 7.

Treatment	Norm. mean specific EROD activity	Standard deviation (+-)
BaP 0.1 µM	1.00	0.26
BaP 0.1 µM + BM 2.5 µM	2.37	0.56
BaP 0.1 µM + HYC 2.5 µM	2.22	0.70
BaP 0.1 µM + PRD 2.5 µM	1.33	0.51
BaP 0.5 µM	2.40	0.57
BaP 0.5 µM + BM 2.5 µM	5.90	0.80
BaP 0.5 µM + HYC 2.5 µM	3.74	0.56
BaP 0.5 µM + PRD 2.5 µM	3.82	1.69
BNF 0.1 µM	1.00	0.41
BNF 0.1 µM + BM 2.5 µM	2.18	0.97
BNF 0.1 µM + HYC 2.5 µM	2.01	1.38
BNF 0.1 µM + PRD 2.5 µM	2.48	1.74
BNF 0.5 µM	11.32	6.26
BNF 0.5 µM + BM 2.5 µM	42.38	11.56
BNF 0.5 µM + HYC 2.5 µM	27.73	9.15
BNF 0.5 µM + PRD 2.5 µM	23.76	6.25

Table B1: Statistical analysis of datasets from the experiment(s) depicted in Figure 7, applying the Wilcoxon test (95% confidence interval).

#	Treatment 1 (Replicates)	Treatment 2 (Replicates)	p- value (Wilcoxon-test)
1	BM 2.5 µM (12)	HYC 2.5 µM (12)	0.32
2	BM 2.5 µM (12)	PRD 2.5 µM (12)	0.06
3	HYC 2.5 µM (12)	PRD 2.5 µM (12)	0.001
4	BM 2.5 µM (12)	HYC 2.5 µM (12)	0.59
5	BM 2.5 µM (12)	PRD 2.5 µM (12)	0.24
6	HYC 2.5 µM (12)	PRD 2.5 µM (12)	0.62
7	BaP 0.1 µM + BM 2.5 µM (16)	BaP 0.1 µM + HYC 2.5 µM (16)	0.38
8	BaP 0.5 µM + HYC 2.5 µM (16)	BaP 0.5 µM + PRD 2.5 µM (16)	0.18
9	BNF 0.1 µM + BM 2.5 µM (12)	BNF 0.1 µM + HYC 2.5 µM (12)	0.20
10	BNF 0.1 µM + BM 2.5 µM (12)	BNF 0.1 µM + PRD 2.5 µM (12)	0.72
11	BNF 0.1 µM + HYC 2.5 µM (12)	BNF 0.1 µM + PRD 2.5 µM (12)	0.62
12	BNF 0.5 µM + HYC 2.5 µM (12)	BNF 0.5 µM + PRD 2.5 µM (12)	0.27
13	BaP 0.1 µM (16)	BaP 0.1 µM + BM 2.5 µM (16)	$7.4*10^{-7}$
14	BaP 0.1 µM (16)	BaP 0.1 µM + HYC 2.5 µM (16)	$3.0*10^{-8}$
15	BaP 0.1 µM (16)	BaP 0.1 µM + PRD 2.5 µM (16)	$4.5*10^{-3}$
16	BaP 0.5 µM (16)	BaP 0.5 µM +BM 2.5 µM (16)	$7.4*10^{-7}$
17	BaP 0.5 µM (16)	BaP 0.5 µM + HYC 2.5 µM (16)	$1.41*10^{-5}$
18	BaP 0.5 µM (16)	BNF 0.5 µM + PRD 2.5 µM (8)	$4.51*10^{-3}$
19	BNF 0.1 µM (12)	BNF 0.1 µM + BM 2.5 µM (8)	$1.87*10^{-5}$
20	BNF 0.1 µM (12)	BNF 0.1 µM + HYC 2.5 µM (8)	0.03
21	BNF 0.1 µM (12)	BNF 0.1 µM + PRD 2.5 µM (8)	0.02
22	BNF 0.5 µM (12)	BNF 0.5 µM + BM 2.5 µM (8)	$6.7*10^{-9}$
23	BNF 0.5 µM (12)	BNF 0.5 µM + HYC 2.5 µM (8)	$1.24*10^{-6}$
24	BNF 0.5 µM (12)	BNF 0.5 µM + PRD 2.5 µM (8)	$8.94*10^{-6}$

Figure 8

Table C: Normalized mean EROD activity as depicted in Figure 8.

Treatment	Norm. mean specific EROD activity	Standard deviation (+-)
BaP 0.1 µM	1.00	0.13
BaP 0.1 µM + DEX 2.5 µM	1.62	0.14
BaP 0.1 µM	1.00	0.53
BaP 0.1 µM + DEX 2.5 µM	1.38	0.10
BaP 0.1 µM	1.00	0.02
BaP 0.1 µM + DEX 2.5 µM	1.15	0.40
BaP 0.1 µM	1.00	0.28
BaP 0.1 µM + DEX 2.5 µM	1.32	0.09
BaP 0.1 µM	1.00	0.10
BaP 0.1 µM + DEX 2.5 µM	0.99	0.12

Table C1: Statistical analysis of datasets from the experiment(s) depicted in Figure 8, applying the Wilcoxon test (95% confidence interval).

#	Treatment 1 (Replicates)	Treatment 2 (Replicates)	p- value (Wilcoxon-test)
1*	BaP 0.1 µM (4)	BaP 0.1 µM + DEX 2.5 µM (4)	0.11
2*	DMSO (4)	BaP 0.1 µM + DEX 2.5 µM (4)	0.34
3*	DMSO (4)	BaP 0.1 µM (4)	0.20
4*	DEX 2.5 µM (4)	BaP 0.1 µM + DEX 2.5 µM (4)	0.89
5	BaP 0.1 µM (4)	BaP 0.1 µM + DEX 2.5 µM (4)	1.00

* Not displayed

Figure 9

Table D: Normalized mean EROD activity as depicted in Figure 9.

Treatment	Exposure Time [h]	Norm. mean specific EROD activity	Standard deviation (+-)
BaP 0.1 µM	48	1.00	0.21
BaP 0.1 µM + DEX 2.5 µM	48 + 24	2.02	0.54
BaP 1.0 µM	48	1.14	0.28
BaP 1.0 µM + DEX 2.5 µM	48 + 24	0.34	0.20
BaP 0.1 µM	48	1.00	0.18
BaP 0.1 µM + DEX 2.5 µM	24 + 48	0.98	0.18
BaP 1.0 µM	48	1.05	0.31
BaP 1.0 µM + DEX 2.5 µM	24 + 48	0.95	0.43

Table D1: Statistical analysis of datasets from the experiment(s) depicted in Figure 9, applying the Wilcoxon test (95% confidence interval).

#	Treatment 1 (Replicates)	Treatment 2 (Replicates)	p- value (Wilcoxon - test)
1	BaP 0.1 µM (8)	BaP 1 µM (8)	0.24
2	BaP 0.1 µM (8)	BaP 0.1 µM + DEX 10 µM (8)	$1.55*10^{-4}$
3	BaP 1 µM (8)	BaP 1 µM + DEX 10 µM (8)	$3.11*10^{-4}$
4	BaP 0.1 µM (8)	BaP 1 µM (8)	0.89
5	BaP 0.1 µM (8)	BaP 0.1 µM + DEX 10 µM (8)	0.65
6	BaP 1 µM (8)	BaP 1 µM + DEX 10 µM (8)	0.80

Figure 10

Table E: Normalized mean EROD activity as depicted in Figure 10.

Treatment	Exposure Time [h]	Norm. mean specific EROD activity	Standard deviation (+-)
BNF 0.1 µM	48	0.80	0.16
BNF 0.1 µM + DMSO	48 + 24	1.00	0.60
BNF 0.1 µM + DEX 0.625 µM	48 + 24	0.75	0.40
BNF 0.1 µM + DEX 1.25 µM	48 + 24	2.42	0.51
BNF 0.1 µM + DEX 2.5 µM	48 + 24	1.94	0.67
BNF 0.1 µM + DEX 5 µM	48 + 24	3.11	1.08
BNF 0.1 µM + DEX 10 µM	48 + 24	1.52	0.56
BNF 0.1 µM + DMSO	48+ 0.17	1.00	0.23
BNF 0.1 µM + DEX 0.625 µM	48 + 0.17	0.49	0.14
BNF 0.1 µM + DEX 1.25 µM	48+ 0.17	0.84	0.26
BNF 0.1 µM + DEX 2.5 µM	48 + 0.17	0.78	0.27
BNF 0.1 µM + DEX 5 µM	48+ 0.17	0.87	0.42
BNF 0.1 µM + DEX 10 µM	48 + 0.17	0.46	0.15

Table E1: Statistical analysis of datasets from the experiment(s) depicted in Figure 10, applying the Wilcoxon test (95% confidence interval).

#	Treatment 1 (Replicates)	Treatment 2 (Replicates)	p- value (Wilcoxon-test)
1	BNF 0.1 µM + DMSO	BNF 0.1 µM	1.00
2	BNF 0.1 µM + DMSO	BNF 0.1 µM + DEX 0.625 µM	0.49
3	BNF 0.1 µM + DMSO	BNF 0.1 µM +DEX 10 µM	0.34
4	BNF 0.1 µM + DMSO	BNF 0.1 µM + DEX 1.25 µM	0.43
5	BNF 0.1 µM + DMSO	BNF 0.1 µM + DEX 2.5 µM	0.32
6	BNF 0.1 µM + DMSO	BNF 0.1 µM + DEX 5 µM	0.56

Figure 11

Table F: Normalized mean CYP1A mRNA activity as depicted in Figure 11.

Treatment	Exposure Time [h]	Norm. CYP1A mRNA level	Standard deviation (+-)
DMSO	24	0.05	0.00
BaP 0.1 µM	24	511.13	47.15
DEX 2.5 µM	24	0.87	0.02
DEX 5 µM	24	0.14	0.001
BaP 0.1 µM + DEX 2.5 µM	24	264.81	6.24
BaP 0.1 µM + DEX 5 µM	24	219.31	5.75
BaP 0.1 µM	3	921.40	3.07
DEX 2.5 µM	3	2.19	0.05
BaP 0.1 µM + DEX 2.5 µM	3	1174.98	28.28

Figure 12

Table G: Normalized mean intracellular BaP level as depicted in Figure 12.

Treatment	Exposure Time [h]	Norm. BaP level
BaP 0.1 µM	1	1.00
BaP 0.1 µM + DEX 2.5 µM	1	1.03
BaP 0.1 µM	24	1.00
BaP 0.1 µM + DEX 2.5 µM	24	0.72
BaP 1 µM	1	1.00
BaP 1 µM + DEX 2.5 µM	1	1.96
BaP 1 µM	6	1.00
BaP 1 µM + DEX 2.5 µM	6	3.11
BaP 1 µM	24	1.00
BaP 1 µM + DEX 2.5 µM	24	1.68